Institutional Asset Pricing with Segmentation and Household Heterogeneity*

Goutham Gopalakrishna[†] Zhouzhou Gu[‡] Jonathan Payne[§]

September 29, 2025

Abstract

How does the organization of the financial sector impact different households? To answer this question, we build a heterogeneous agent model with households facing asset market participation constraints, banks providing deposits, funds providing insurance/pension products, and endogenous asset price volatility. We solve the model globally by developing a new deep learning methodology for macro-finance models and calibrate the model to asset pricing dynamics and household portfolio choices. Counterfactual experiments reveal distinct trade-offs. Regulatory interventions increase stability but at the expense of lower growth and higher wealth inequality. Demographic shifts compress inequality but reduce aggregate wealth, showing how regulation and demographics jointly shape the interaction of asset prices, stability, and the wealth distribution.

Keywords: Market Segmentation, Asset Pricing, Heterogeneous Agent Macroeconomic Models, Deep Learning, Inequality.

JEL: C63, C68, E27, G12, G21, G22, G23

*This paper was previously circulated as "Asset Pricing, Participation Constraints, and Inequality". We are very grateful to the comments and discussion from Jaroslav Borovička, Anmol Bhandari, Markus Brunnermeier, Paul Ehling (Discussant), Lars Hansen, Felix Kubler, Richard Rogerson, Martin Schneider, Yucheng Yang, Moto Yogo, Jan Žemlička, and Adam Zhang (Discussant). We thank Yulong Peng for an excellent research assistance. We are also thankful for the comments from participants in the NBER SI, CESifo Conference, Blue Collar Working Group at the University of Chicago, the Workshop on the Frontier of Quantitative Macroeconomics: Methods and Models, and the 2024 SED.

[†]University of Toronto, Rotman School of Management. Email: goutham.gopalakrishna@rotman.utoronto.ca

[‡]Princeton, Department of Economics. Email: zg3990@princeton.edu

[§]Princeton, Department of Economics. Email: jepayne@princeton.edu

1 Introduction

Households rely on financial intermediaries for a wide range of services, including access to asset markets, life insurance, retirement pensions, deposits, and credit. Extensive research has shown that providing these services is complicated: institutional and regulatory constraints restrict intermediary behavior leading to price distortions and endogenous price volatility (e.g. Koijen and Yogo (2019, 2023)). This has broad implications for household welfare because it influences how effectively different households can share risk and access high returns, which ultimately shapes with distribution of wealth in the economy. In this paper we study these macroeconomic connections and show how policy makers face important and subtle tradeoffs between managing stability, growth, and inequality.

There are three main contributions of this paper. First, we develop a novel quantitative heterogeneous-agent model that embeds intermediary asset pricing into a general equilibrium model with a non-degenerate wealth distribution. Second, while prior work emphasizes how intermediary frictions drive asset pricing phenomena, we show how these frictions endogenously map into wealth and consumption inequality across households. Third, we develop a deep-learning solution method that delivers global solutions in environments with aggregate risk, stochastic volatility, and binding portfolio constraints—settings where standard numerical methods fail. Together, these innovations allow us to bridge the intermediary asset pricing and macroeconomics literatures and to quantify the distributional consequences of regulatory segmentation of financial institutions. We calibrate the model to the post-financial crisis period and conduct counterfactual experiments that examine alternative regulatory and demographic regimes.

In Section 2, we study a heterogeneous agent real business cycle model with financial intermediaries and endogenous asset price volatility. There are two mean-reverting aggregate shock processes in the economy: the level of capital productivity and the volatility of capital productivity. The economy is populated by price-taking households who have inelastic or restricted demand for different assets. Households face idiosyncratic death shocks, which lead to demand for long-duration insurance or pension products, similar to the "preferred habitat" demand in Vayanos and Vila (2021). Households also face costs when participating in the capital market. This leads to heterogeneous household portfolio choices, with wealthier households having greater exposure to capital, and ultimately, a non-degenerate household wealth distribution. The economy also contains two types of financiers who provide financial services to households: bankers who issue deposits and fund managers who issue long-duration insurance/pension products. Neither type of financier can raise equity.[1]

[1] The model can be extended naturally to an environment where financial intermediaries can raise a limited

Finally, there is a government that issues long-term bonds and raises wealth taxes. The financial frictions on the households and financial intermediaries mean that the agent wealth distribution impacts the capital, insurance, and government bond price processes.

In Section 3, we present a deep-learning algorithm to solve the model. In Section 4, we calibrate our baseline model to the post-financial crisis period (2010Q1 to 2024Q4) and show that the model does a good job of matching asset pricing, macroeconomic, and household portfolio moments. The portfolio constraints generate heterogeneous capital holdings, while annuity holdings are near-homogeneous due to the preferred habitat nature of demand. The central friction is that banks do not internalize their price impact and therefore take on high leverage, which amplifies endogenous volatility in asset prices and returns and, ultimately, household consumption volatility. The combination of heterogeneous risk exposures of households and endogenous returns generates a fat-tailed household wealth distribution with rich cross-sectional portfolio moments that are consistent with the data. The interaction between intermediaries plays a central role: funds act as risk absorbers by expanding capital holdings during TFP recessions, purchasing assets that banks shed. This behavior arises because fund liabilities (annuities) fall in value during recessions, while banks liabilities (deposits) value remain unaffected. As a result, funds gain wealth during recessions, purchasing assets from other agents, stabilizing the capital market. But this comes at the cost of charging high prices on annuities, affecting household wealth.

In Sections 5 and 6, we conduct three counterfactual experiments. First, we impose bank-style leverage restrictions on funds. In this "fund-regulated" economy, funds shrink their balance sheets by holding less capital and issuing fewer annuities. Because banks are already constrained, households fill the vacuum by increasing their capital holdings and reducing annuity demand. Aggregate financial-sector capital holdings fall, raising expected returns, dampening endogenous volatility, and reducing output and investment. Households benefit from lower consumption volatility but face higher inequality, since richer households capture a disproportionate share of the elevated returns.

Second, we tighten bank leverage requirements, reflecting concerns that current restrictions remain too lax (Admati and Hellwig, 2013). In this "bank-regulated" economy, banks further contract their capital holdings, and funds expand to fill the gap. With larger balance sheets, funds strengthen their role as shock absorbers and issue more annuities at attractive prices. However, their expansion increases endogenous capital price volatility, raising household consumption risk relative to the fund-regulated case. Inequality again rises, as wealthier households benefit disproportionately from wider capital return spreads. Together, these experiments highlight the trade-offs between stability, macroeconomic outcomes, and

quantity of outside equity.

distributional consequences.

Finally, we study a "demographic" counterfactual with a higher household death rate. This shift produces surprising sectoral reallocations: heightened demand for annuities and capital pushes up prices to the point where return spreads turn negative. Funds retreat from the capital market, shrinking their balance sheets, and households are left with fewer annuities precisely when mortality risk is highest. Banks expand through higher leverage and assume the role of stabilizers in the capital market. Output and investment rise as more capital is held by banks, but household wealth and consumption fall. The wealth distribution compresses, as capital is more evenly spread across households, lowering inequality at the expense of lower aggregate wealth and higher risk exposure.

Literature Review: We contribute to several strands of literature. The first is the macro-finance literature studying how financial institutions generate endogenous risk in dynamic general equilibrium models (Brunnermeier and Sannikov, 2014; He and Krishnamurthy, 2013; Krishnamurthy and Li, 2020; Maxted, 2023; Gertler, Kiyotaki and Prestipino, 2019). These papers highlight the role of financial intermediaries in amplifying aggregate shocks, typically focusing on sectoral heterogeneity between households and intermediaries. More recent work introduces heterogeneity across intermediaries themselves (Kargar, 2021; Coimbra and Rey, 2024), emphasizing the dynamics of financial cycles. Our contribution relative to this literature is to combine intermediary heterogeneity with household wealth distribution, thereby producing rich cross-sectional outcomes for households and sector-level outcomes between the intermediaries.

Secondly, we are part of an active literature studying how asset pricing can impact the household wealth distribution (recent examples include Gomez (2017), Cioffi (2021), Gomez and Gouin-Bonenfant (2024), Fagereng, Gomez, Gouin-Bonenfant, Holm, Moll and Natvik (2022), Basak and Chabakauri (2024), Fernández-Villaverde and Levintal (2024), Irie (2024) amongst many others). This work builds on ample empirical evidence documenting the heterogeneity in household portfolio choices and asset returns (Bach, Calvet and Sodini (2020), Fagereng, Guiso, Malacrino and Pistaferri (2020), Catherine, Miller, Paron and Sarin (2022), Bricker, Volz and Hansen (2018), etc.). Our model extends this literature by endogenizing both capital market participation and price volatility in a heterogeneous-agent macro-finance environment with multiple intermediaries and portfolio choice over long-lived assets. In doing so, we connect to the literature on limited financial market participation affecting asset prices (Gomes and Michaelides (2007), Guvenen (2009), Favilukis (2013),Lansing (2015), Vayanos and Vila (2021), Khorrami (2021), Gaudio, Petrella and Santoro (2023), Gaudio (2024), etc.). A smaller but growing line of work incorporates pensions into macro-finance models. For instance, Coimbra and Rey (2024) embeds defined-benefit pension funds in an incomplete-markets framework to explain the equity premium. Our contribution is to integrate pension and insurance sectors directly into a DSGE model with financial amplification, thereby linking regulatory regimes to asset pricing and distributional outcomes. This connects to empirical work showing that regulation of financial institutions and institutional investors influences asset prices (Greenwood and Vissing-Jorgensen, 2018).

Finally, we speak to the computational economics literature employing deep learning to solve complex heterogeneous-agent models that challenge traditional solution techniques (Azinovic, Gaegauf and Scheidegger, 2022; Han, Yang and E, 2021; Maliar, Maliar and Winant, 2021; Kahou, Fernández-Villaverde, Perla and Sood, 2021; Bretscher, Fernández-Villaverde and Scheidegger, 2022; Fernández-Villaverde, Marbet, Nuño and Rachedi, 2023a; Han, Jentzen and E, 2018; Huang, 2022; Duarte, Duarte and Silva, 2024; Gopalakrishna, 2021; Fernández-Villaverde, Hurtado and Nuño, 2023b; Sauzet, 2021; Gu, Laurière, Merkel and Payne, 2023). While several papers apply deep learning to heterogeneous-agent models with portfolio choice between short-term risky assets (Fernández-Villaverde, Hurtado and Nuno, 2023; Huang, 2023), only a few tackle long-term asset pricing in general equilibrium. For example, Azinovic and Žemlička (2023) solve a discrete-time model with long-lived assets by encoding equilibrium conditions directly into neural networks, employing low-dimensional approximations of the wealth distribution in the spirit of Kubler and Scheidegger (2018). A central challenge is that pricing long-term assets requires solving simultaneously for equilibrium allocations and individual choices, as emphasized by Guvenen (2009). Our contribution is to demonstrate that in continuous time, working directly in the wealth share space, these equilibrium objects can be determined globally in a unified framework. Methodologically, we show how to solve macro-finance models with heterogeneous intermediaries, long-lived assets, and rich wealth distributions without resorting to restrictive approximations.

The rest of this paper is structured as follows. Section 2 outlines our economic model. Section 3 introduces our numerical algorithm. Section 4 describes the calibration of the baseline model. Section 5 and 6 presents counterfactual experiments before concluding.

2 Baseline Economic Model

In this section, we outline the economic model used throughout the paper. We study a continuous time stochastic production economy with heterogeneous households who face retirement shocks and asset market participation constraints. The households are serviced by two types of representative financial intermediaries: a banker that accepts deposits and makes loans, and a fund manager that offers pensions to insure the retirement shocks.

2.1 Environment

Setting: The model is in continuous time with an infinite horizon. There is a perishable consumption good and a durable capital stock. The economy is populated by a unit continuum of price-taking households (h), indexed by $i \in [0,1]$, a unit continuum of price-taking bankers (b), and a unit continuum of price-taking funds (f) that we interpret as the combined pension and insurance sector. The banking and fund sectors will each aggregate to pseudo representative agents but the household sector will not. The economy has the following assets: short-term bank deposits, fund contracts, bank loans, capital stock, and government bonds.

Production: There is a production technology that creates consumption goods according to the linear production function $Y_t = e^{z_t} k_t$ where k_t is the capital used at time t and z_t is aggregate productivity that evolves according to:

$$dz_t = \beta_z(\bar{z} - z_t)dt + \sigma_z dW_{z,t},$$

where $W_{z,t}$ denotes the aggregate Brownian motion process. All agents can create capital stock using an investment technology that converts $\iota_t k_t$ goods into $\phi(\iota_t)k_t$ capital, where ι_t is referred to as the investment rate. Capital depreciates at rate $\delta >$ So, an agent's physical capital stock evolve according to:

$$dk_t = (\phi(\iota_t)k_t - \delta k_t)dt.$$

Households: There is a unit measure of households who follow a life cycle. Households are born as "young" agents and then transition to "retired" agents at rate λ_h. While young, agents have discount rate ρ_h and get flow utility $u(c_{h,t}) = \beta c_{h,t}^{1-\gamma}/(1-\gamma)$ from consumption $c_{h,t}$. When households retire, they disengage from the productive sector and consume their remaining wealth. We follow the macro-finance literature and model this by assuming that households receive a lump sum of utility $\mathcal{U}(\mathcal{C}_{h,t}) = (1-\beta)\mathcal{C}_{h,t}^{1-\Gamma}/(1-\Gamma)$ from consuming a lump sum of consumption $\mathcal{C}_{h,t}$ at retirement. After one household retires, it is immediately replaced by a new young household who receives initial wealth $\underline{a}_{h,t} = \phi_h A_t$, where A_t is the total wealth in the economy.

Households face two financial frictions. First, they face a "participation friction" that holding capital stock incurs the flow cost:

$$\Psi_{h,k}(k_{h,t}, a_{h,t}) = \psi_{h,k,t}\Xi_{h,t}a_{h,t}, \text{ where } \psi_{h,k,t} = \psi_h(\theta^k_{h,t}, \eta_{h,t}) = \frac{\bar{\psi}_k}{2\eta_{h,t}}\left(\theta^k_{h,t}\right)^2$$

where $\bar{\psi}_k$ is the severity of the constraint, $\theta^k_{h,t}$ is the household's share of wealth in capital, $\eta_{h,t}$ is the household's share of wealth in the economy, and $\Xi_{h,t}$ is the equilibrium stochastic discount factor of the household. The constraint imposes that wealthier agents have better direct access to production opportunities and is interpreted as capturing the fixed costs or cognitive constraints with direct entrepreneurship. Second, households cannot write contracts with each other to insure against retirement shocks. This generates a "preferred-habitat" style need for financial intermediaries that can provide pension/insurance products with average maturity λ_h.

Financial intermediaries: There are two types of financial intermediaries: bankers (b) and fund managers (f). Each type of intermediary $j \in \{b, f\}$ has discount rate ρ_j and gets flow utility $u_j(c_{j,t}) = c_{j,t}^{1-\gamma_j}/(1-\gamma_j)$ from consuming $c_{j,t}$ flow goods. The intermediaries differ in what type of liabilities they issue. Bankers only issue risk-free short-term deposits that pay a deposit rate r^d_t. Fund managers only sell contracts to households that pay one good to the holder when they die so it can interpreted as a combination of a life-insurance and a pension product. On the asset side of the balance sheet, both banks and fund managers can hold capital and government bonds subject to any regulatory frictions described below. Financial intermediaries of type $j \in (b, f)$ exit at rate λ_j and are replaced by new financial intermediaries with initial wealth $\underline{a}_{f,t} = \phi_f A_t$. Ultimately, both banker and fund manager policies will be independent of wealth so we can replace the continuum of bankers and funds by a representative banker and fund.

Government: The government issues zero coupon bonds that mature at rate λ_m and pay 1 unit of consumption good at maturity. We impose that bond supply is Mk_t. The government raises flow wealth taxes to finance the issuance of debt and redistribute wealth to the new entrants in the economy, which could equivalently be decentralized as an inheritance system. We let τ_j denote the flow wealth tax on an agent of type $j \in \{h, b, f\}$.

In addition to its fiscal policy, the government also imposes regulatory constraints on the financial sector. Financial intermediaries of type $j \in \{b, f\}$ face the portfolio penalties that:

$$\Psi_{j,l}(k_{j,t}, a_{j,t}) = \psi_{j,l,t}\Xi_{j,t}a_{j,t}, \text{ where } \psi_{j,l,t} = \frac{\psi^l_j}{2}\left[\min\{0, \theta^l_{j,t}\}^2 + \max\{0, \theta^l_{j,t} - \bar{\theta}^l_{j,t}\}^2\right], \quad l \in \{k, m\}$$

where $\bar{\theta}_{j,l}$ is the regulatory target portfolio share for agent j in asset l, and ψ^l_j is the tightness of the regulatory requirement. The institutions also face a penalty for shorting to mimic a short-selling constraint.

Assets, markets, and financial frictions: Each period, there are competitive markets for goods and capital trading. We use goods as the numeraire. Let r_t^d denote the interest rate on deposits and let $\boldsymbol{q}_t := (q_t^k, q_t^n, q_t^m)$ denote a vector with the price of capital, pension shares, and government bonds respectively. We guess and verify that for each asset $l \in \{k, n, m\}$ the long-term price process satisfies:

$$\frac{dq_t^l}{q_t^l} = \mu_{q^l,t}dt + \sigma_{q^l,t}dW_t,$$

where $\mu_{q^l,t}$ and $\sigma_{q^l,t} := \sigma_{q^l,z,t}$ are the drift and volatility for asset $l \in \{k, n, m\}$. We also express the return processes by:

$$\begin{aligned}
dR_t^k &= r_t^k dt + \sigma_{q^k,t}dW_t, & r_t^k &:= \mu_{q^k,t} + \Phi(\iota) - \delta + \frac{e^{z_t} - \iota}{q_t^k}, \\
dR_{h,t}^n &= r_{h,t}^n dt + \sigma_{q^n,t}dW_t + \frac{1}{q_t^n}dN_{h,t}, & r_{h,t}^n &:= \mu_{q^n,t} \\
dR_{f,t}^n &= r_{f,t}^n dt + \sigma_{q^n,t}dW_t, & r_{f,t}^n &:= \mu_{q^n,t} + \left(\frac{1}{q_t^n} - 1\right)\lambda_h \\
dR_t^m &= r_t^m dt + \sigma_{q^m,t}dW_t & r_t^m &:= \mu_{q^m,t} + \left(\frac{1}{q_t^m} - 1\right)\lambda_m
\end{aligned}$$

where annuities have different flow returns for the household, $R_{h,t}^n$, and fund, $R_{f,t}^n$, because the fund aggregates across a continuum of households.

2.1.1 Discussion of Key Environmental Features

This environment has been constructed to nest a collection of models and economic forces commonly studied in the literature. We discuss these connections below:

(i) *Preferred habitat literature:* If we set $\beta = 0$ so the households only care about consumption at retirement and set $\mathcal{U}(\cdot)$ to be either the Type I or Type II agents from the Appendix in Vayanos and Vila (2021), then our households reduce to the "preferred habitat agents" in Vayanos and Vila (2021) who only demand maturities with average maturity $1/\lambda_h$.[2] However, our model has an important extension compared to the preferred habitat literature—we integrate the preferred habitat demand into a standard portfolio choice problem so that overall household demand is a combination of the "preferred-habitat" component and a standard portfolio choice problem that

[2]In order to generate the full yield curve model in Vayanos and Vila (2021), we would also need to introduce variation in λ_h across households and bonds with different average maturities.

balances risk and return. This allows us to understand how risk and inelastic demand interact in a general equilibrium model.

(ii) *Perpetual youth literature:* If we set $\beta = 1$ so the households only care about consumption while young, then we recover the perpetual youth model from Blanchard (1985). In this case, households demand annuities that pay until they die, which the households could recreate synthetically by shorting the life insurance products offered by the funds and purchasing bonds. In this sense, the two extreme parameterizations, $\beta \in \{0, 1\}$, nest the two most commonly used models of demand for pension/insurance products: preferred habitat and perpetual youth. Our model can be viewed as an intermediate model that nests these two forces. Throughout the paper we focus on parametrizations where the households take long positions in the fund contracts. However, the model could just as easily be solved for the case where the CES is linear and some households end up shorting the pension products.

(iii) *Participation constraint models:* We have set up the household participation penalty so that households increase their fraction of wealth in capital as get older. In this sense, as household wealth becomes small (or the participation penalty becomes infinitely large), the model becomes the Basak and Cuoco (1998) environment in which households cannot participate in the capital market. However, as household wealth becomes large (or the participation penalty becomes zero), the agents become unconstrained like in the Brunnermeier and Sannikov (2014) environment where households can freely participate in the capital market. At either extreme, household portfolio choices become homogeneous and the household sector aggregates. The technical difficulties come from having the household move between the extremes as they accumulate wealth.

(iv) *Different type models (e.g. Chan and Kogan (2002), Gomez (2017)):* There is a collection of models in which households have different types ex-ante (e.g. because they have heterogeneous risk aversion) but all agents within a particular type make the same portfolio decisions. These models can generate heterogeneous portfolio choices across the different types in the population and so can generate the aggregate asset portfolio for the household sector. However, they cannot match any of the portfolio data at the micro level, which shows that portfolio decisions vary with household wealth.

2.2 Equilibrium

We now setup the agent problems and equilibrium. We let $a_{j,t}$ denote the wealth of a type $j \in \{h, b, f\}$ agent, where the indices h, b, f refer to household, banker and fund manager respectively. So, by definition, $a_{h,t} = q_t^k k_{h,t} + q_t^n n_{h,t} + d_{h,t}$, $a_{b,t} = q_t^k k_{b,t} + q_t^m m_{b,t} + d_{h,t}$, and $a_{f,t} := q_t^k k_{f,t} + q_t^m m_{f,t} + q_t^n n_{f,t}$. We let $\mu_{a_j,t}$ and $\sigma_{a_j,t}$ denote the geometric drift and volatility for the wealth of a type $j \in \{h, b, f\}$ agent. We let $\theta_{j,t}^l = q_t^l l_{j,t}/a_{j,t}$ denote the share of wealth that an agent of type j with wealth $a_{j,t}$ has in asset l and let $\boldsymbol{\theta}_{j,t}$ denote the vector of wealth shares chosen by an agent of type j with wealth $a_{j,t}$ at time t. We use the notation $\mathsf{x} = (x_t)_{t\geq 0}$ to denote the stochastic process for variable x_t and $\tilde{\mathsf{x}}$ to denote an agent belief about the process for x_t.

Household problem: Given their belief about price processes, $(\tilde{\mathsf{r}}, \tilde{\mathsf{q}})$, and initial wealth, $a_{h,0}$, a household chooses consumption, portfolio, and investment processes $(\mathsf{c}_h, \boldsymbol{\theta}_h, \iota_h)$ to solve the Problem (2.1) below:

$$\begin{aligned}
&\max_{\mathsf{c}_h, \boldsymbol{\theta}_h} \mathbb{E}\left[\int_0^T e^{-\rho_h t}\left(u(c_{h,t}) + \psi_{h,k,t}(\theta_{h,t}^k)\Xi_{h,t}a_{h,t} + \psi_{h,d,t}(\theta_{h,t}^d)\Xi_{h,t}a_{h,t}\right)dt + e^{-\rho T}\mathcal{U}(\mathcal{C}_{h,T})\right] \\
&s.t.\ \ \frac{da_{h,t}}{a_{h,t}} = \theta_{h,t}^n d\tilde{R}_{h,t}^n + \theta_{h,t}^k d\tilde{R}_t^k + \left((1 - \theta_{h,t}^k - \theta_{h,t}^n)\tilde{r}_{d,t} - c_{h,t}/a_{h,t} - \tau_{h,t}\right)dt \qquad (2.1) \\
&\qquad \mathcal{C}_{h,T} \leq \left(1 - \theta_{h,t}^n + \frac{\theta_{h,t}^n}{q_t^n}\right)a_{h,t}
\end{aligned}$$

where $\tau_{h,t}$ is the net tax or transfer (per unit of wealth) while agents are alive.

Financial intermediary problems: Given their belief about price processes, $(\tilde{\mathsf{r}}, \tilde{\mathsf{q}})$, and initial wealth, $a_{j,0}$, a financial intermediary of type $j \in \{b, f\}$ chooses their consumption, portfolio, and investment processes $(\mathsf{c}_j, \boldsymbol{\theta}_j, \iota_j)$ to solve the Problem (2.2) below:

$$\begin{aligned}
&\max_{\mathsf{c}_j, \boldsymbol{\theta}_j, \iota_j} \left\{\int_0^\infty e^{-\rho_j t}\left(u(c_{j,t}) + \psi_{j,k}(\theta_{j,t}^k)\xi_{j,t}a_{j,t} + \psi_{j,m}(\theta_{j,t}^m)\xi_{j,t}a_{j,t}\right)dt\right\} \\
&s.t.\ \ \frac{da_{j,t}}{a_{j,t}} = \theta_{j,t}^k d\tilde{R}_t^k + \theta_{j,t}^m d\tilde{R}_t^m + (1 - \theta_{j,t}^k - \theta_{j,t}^m)d\tilde{R}_t^j + (-c_{j,t}/a_{j,t} - \tau_{j,t})\,dt
\end{aligned} \qquad (2.2)$$

where $d\tilde{R}_t^j$ is return on liabilities for type j, which equals $\tilde{r}_t^d dt$ for bankers $j = b$ and $d\tilde{R}_t^n$ for fund managers $j = f$.

Distribution: Throughout this paper, we work with the distribution of wealth shares rather than wealth levels. The bank and fund sectors aggregate so we will only need to track of the aggregate states for each sector. We let $\eta_{b,t} := a_{b,t}/A_t$ and $\eta_{f,t} := a_{f,g}/A_t$ denote the share of aggregate wealth held by the banking and fund sectors. The uninsurable idiosyncratic shocks and wealth dependent differences in household portfolio constraints generate a non-degenerate cross-section distribution of household wealth across the economy. We let $g_{h,t} = \{\eta_{i,t} = a_{i,t}/A_t : i \in \mathcal{I}\}$ denote measure of household wealth shares across the economy at time t for a given filtration $\mathcal{F}_t$, where $\mathcal{F}_t$ is generated the by aggregate shock processes $\{\boldsymbol{W}_t\}_{t\geq 0}$. With some abuse of notation, we let $G = (\eta_{b,t}, \eta_{f,t}, g_{h,t})$ denote the collection of distribution states in the economy.

Definition 1 (Equilibrium)**.** For a given set of government taxation policies, an equilibrium is a collection of $\mathcal{F}_t$-adapted processes $(\mathsf{K}, \mathsf{r}, \mathbf{q}, \mathsf{G})$ and household decision processes $(\mathbf{c}_i, \boldsymbol{\iota}_i, \boldsymbol{\theta}_i)$ for $i \in I$ and financial intermediary decision processes $(\mathbf{c}_i, \boldsymbol{\iota}_i, \boldsymbol{\theta}_i)$ for $j \in \{b, f\}$ such that:

1. Given beliefs $(\tilde{\mathbf{r}}, \tilde{\mathbf{q}})$, households $(i \in I)$ solve Problem 2.1 and financial intermediaries solve Problem 2.2.

2. The price processes $(\mathbf{r}, \mathbf{q})$ satisfies market clearing conditions at each t (where the capital letter $Y_{j,t}$ refers to the aggregate quantity of variable Y held by an agent of type $j \in \{h, b, f\}$):

   (a) Goods market clears: $C_{h,t} + C_{b,t} + C_{f,t} + \lambda_h \mathcal{E}_{h,t} = e^{z_t} K_t - \iota_t K_t$, where K_t is the aggregate capital stock and $\mathcal{E}_{h,t}$ is the aggregate households' expenditure upon retirement.

   (b) Capital market clears: $\sum_{j\in\{b,n\}} K_{j,t} = K_t$

   (c) Annuity market clears: $N_{h,t} + N_{f,t} = 0$

   (d) Deposit market clears: $D_{h,t} + D_{b,t} = 0$

   (e) Bond market clears: $M_{b,t} + M_{f,t} = M$

3. Agent beliefs are consistent with equilibrium $(\tilde{\mathbf{r}}, \tilde{\mathbf{q}}) = (\mathbf{r}, \mathbf{q})$.

2.3 Recursive Characterization of Equilibrium

In this section, we characterize the equilibrium recursively. We denote the finite dimensional aggregate state vector by $\boldsymbol{s} := (z, K, \eta_b, \eta_f)$ and the full aggregate state space by $\boldsymbol{S} := (\boldsymbol{s}, g_h)$. Under the recursive formulation of the problem, agent beliefs about the price process become agent beliefs about the evolution of sector wealth, $(\tilde{\mu}_{\eta,j}, \tilde{\boldsymbol{\sigma}}_{\eta,j})_{j\in\{h,f\}}$, and the evolution of the density of household wealth shares:

$$dg_{h,t}(a) = \tilde{\mu}_g(a, \boldsymbol{S})dt + \tilde{\boldsymbol{\sigma}}_g(a, \boldsymbol{S})^T d\boldsymbol{W}_t$$

For convenience, we also define the state spaces for an individual agent by $\boldsymbol{x} := (a, z, , K, \eta_b, \eta_f)$ and $\boldsymbol{X} := (\boldsymbol{x}, g_h)$. We let $V_j(\boldsymbol{X})$ and $\xi_j(\boldsymbol{X}) := \partial_a V_j(\boldsymbol{X})$ denote the value function and the derivative of the value function for an agent of type $j \in \{h, b, f\}$ with state variable $\boldsymbol{X}$. We let $\mu_{\xi_h}(\boldsymbol{X})$ and $\sigma_{\xi_h}(\boldsymbol{X})$ denote drift and volatility of the process for ξ_j. Theorems 1, 2, and 3 below summarize the recursive characterization of equilibrium. For convenience, we group the characterization into three blocks: (i) the optimization problems of the agents, (ii) the evolution of the distribution, and (iii) market clearing.

Theorem 1 (Block 1: Agent Optimization)**.** *Given the price variables $(r^d, (q^l, r^l, \sigma_{q^l})_{l \in \{k,n,m\}})$, the household variables $(\xi_h, c_h, \boldsymbol{\theta}_h)$ satisfy the Euler equation and FOCs*

$$\begin{aligned}
0 &= -(\rho_h + \lambda_h) + \mu_{\xi_h} + r^d - \tau_h + \psi_{h,k}(\theta_h^k) - \partial_{\theta_h^k}\psi_{h,k}(\theta_h^k)\theta_h^k + \psi_{h,d}(\theta_h^d) - \partial_{\theta_h^d}\psi_{h,d}(\theta_h^d)\theta_h^d \\
0 &= u'(c_h) - \xi_h \\
0 &= \Phi'(\iota) - (q^k)^{-1} \\
0 &= r^k - r^d + \partial_{\theta_h^k}\psi_{h,k} + \sigma_{\xi_h}\sigma_{q^k} \\
0 &= r^n - r^d + \lambda_h \left(\frac{1}{q^n} - 1\right)\frac{\mathcal{U}'(\mathcal{C})}{a\xi_h} + \sigma_{\xi_h}\sigma_{q^n}
\end{aligned}$$

and the financial intermediary variables $(\xi_j, c_j, \boldsymbol{\theta}_j)_{j \in \{b,f\}}$ satisfy analogous conditions (see Appendix A) where the drift and volatility of ξ_j for all $j \in (h, b, f)$ are given by Itô's lemma:

$$\begin{aligned}
\mu_{\xi_j}\xi_j(\boldsymbol{X}) &= (D_x\xi_j(\boldsymbol{X}))^T\boldsymbol{\mu}_x + \frac{1}{2}tr\left\{(\boldsymbol{\sigma}_x \odot \boldsymbol{x})^T(\boldsymbol{\sigma}_x \odot \boldsymbol{x})D_x^2\xi_j(\boldsymbol{X})\right\} + \boldsymbol{\mathcal{L}}_g\xi_j(\boldsymbol{X}) \\
\sigma_{\xi_j}\xi_j &= (\boldsymbol{\sigma}_x \odot \boldsymbol{x})^T D_x\xi_j(\boldsymbol{X})
\end{aligned}$$

where $\boldsymbol{\mathcal{L}}_g\xi_j(\boldsymbol{X})$ denotes the collection of terms with Frechet derivatives of ξ_j w.r.t. g.

Proof. See Appendix A. □

Combining the first two lines in each agent's system yields the continuous-time Euler equation for the agent's marginal value of wealth. The third line equates the marginal benefit of investment to its marginal cost. The remaining first-order conditions equate each asset's excess return to risk tastes plus wedges generated by financial frictions and additional preference-based features. This captures the standard trade-off between earning an expected return, $r^l - r^d$, and co-movement between the household's stochastic discount factor and price of asset l, $\sigma_{\xi_h}^T \sigma_{q^l}$. They also capture the distortions from the household retirement consumption demand and portfolio constraints. For example, if we rearrange the demand for fund contracts and use the exponential form of the Vayanos and Vila (2021) preferences for the retirement utility, then we get:

$$\underbrace{\lambda_h \left(\frac{1}{q_t^n} - 1\right) \exp\left(-\frac{q_t^k}{q_t^n}\theta_i^n \eta_i\right)}_{\substack{\text{“Preferred habitat”} \\ \text{component}}} = -\underbrace{\left(r_{h,t}^n - r_t^d\right)}_{\substack{\text{Excess} \\ \text{return}}} - \underbrace{\sigma_{\xi_h}\sigma_{q_t^n}}_{\text{“risk shifter”}}$$

which can be interpreted as a generalization of the preferred habitat demand function from Vayanos and Vila (2021). Like Vayanos and Vila (2021), we have the “inelastic” preferred habitat term coming from the need for assets with duration λ_h (the LHS in equation (2.3)). However, instead of exogenous demand shifters, we instead have that the household's risk-return tradeoff (the RHS in equation (2.3)) shift household demand.

Given the individual optimal decisions, we proceed to study how the distribution evolves over time. For the bank and fund sectors, we only need to keep track of the aggregate wealth share dynamics because we can aggregate within each of those sectors. However, for the household sector, the capital market participation constraint generates portfolio heterogeneity and so prevents aggregation. This means that we need to keep track of the full distribution of household wealth. We summarize this in Proposition 2 below.

Theorem 2 (Block 2: Distribution evolution)**.** *Given prices and price processes $(r^d, (q^l, r^l, \boldsymbol{\sigma}_{q^l})_{l \in \{k,n,m\}})$ and agent decisions $(\xi_j, c_j, \boldsymbol{\theta}_j, \iota)_{j \in \{h,b,f\}}$, we can characterize the distribution evolution. At the sector level, the wealth share for financial intermediary $j \in \{b, f\}$ evolves according to:*

$$\frac{d\eta_{j,t}}{\eta_{j,t}} = \left(\mu_{A_j,t} - \mu_{A,t} + (\sigma_{A,t} - \sigma_{A_j,t})\sigma_{A,t}\right) dt + (\sigma_{A_j,t} - \sigma_{A,t}) dW_t \tag{2.3}$$

where:

$$\begin{aligned}
\mu_{A_b,t} &= r^d + \theta_h^k (r^k - r^d) - (\rho_b + \lambda_b) - \tau_b + \lambda_b \left(\phi_b \eta_{b,t}^{-1} - 1\right) \\
\mu_{A_f,t} &= r^b + \theta_f^k (r^k - r_f^b) + \theta_f^m (r^m - r_f^n) - (\rho_f + \lambda_f) - \tau_f + \lambda_f \left(\phi_f \eta_{f,t}^{-1} - 1\right) \\
\mu_{A,t} &= \vartheta_t (\mu_{q^k} + \Phi(\iota) - \delta) + (1 - \vartheta_t)\mu_{q^m}
\end{aligned}$$

and where aggregate wealth is given by $A_t = q_t^k K_t + q_t^m M$ and the aggregate wealth in capital is $\vartheta_t := q_t^k K_t / (q^k K_t + q^m M)$. Within the household sector, the density of household wealth *shares evolves according to:*

$$
\begin{aligned}
dg_{h,t}(\eta) = \Bigg(& \lambda_h \phi(\eta) - \lambda_h g_{h,t}(\eta) - \partial_\eta [\mu_\eta(\eta, \boldsymbol{s}_t, g_{h,t}) g_{h,t}(\eta)] \\
& + \frac{1}{2}\partial_\eta \left[(\sigma^2_{\eta,z}(\eta, \boldsymbol{s}_t, g_{h,t}) + \sigma^2_{\eta,\zeta}(\eta, \boldsymbol{s}_t, g_{h,t})) g_{h,t}(\eta) \right] \Bigg) dt \\
& - \partial_\eta [\sigma_{\eta,z}(\eta, \boldsymbol{s}_t, g_{h,t}) g_{h,t}(\eta)] dW_{z,t}
\end{aligned}
$$

where:

$$
\begin{aligned}
\mu_{\eta_i,t} &= \mu_{a_i,t} - \mu_{A,t} + (\sigma_{A,t} - \sigma_{a_i,t})\sigma_{A,t} \\
\sigma_{\eta_i,t} &= \sigma_{a_i,t} - \sigma_{A,t}
\end{aligned}
$$

Proof. See Appendix A. □

Proposition 2 shows that the distribution evolution equations are directly exposed to the aggregate shock process, $dW_{z,t}$, and so the distributional dynamics in the economy follow a *stochastic Kolmogorov Forward Equation (KFE)*. This is because all economic agents have a direct heterogeneous exposure to the fundamental shock through the instantaneous asset price responses. By contrast, many classic models in the heterogeneous agent macroeconomics literature (e.g. the continuous time version Krusell and Smith (1998) described in Gu et al. (2023)) do not have stochastic KFEs because the aggregate shocks do not directly impact household wealth.

Theorem 3 (Block 3: Market clearing and belief consistency)**.** *The equilibrium prices satisfy:*

$$
\begin{aligned}
\int c_h g_h(\eta) d\eta + \frac{C_b}{A_b}\eta_b + \frac{C_f}{A_f}\eta_f + \lambda_h \int \mathcal{E}_h g_h(\eta) d\eta &= \frac{(e^z - \iota)K}{q^k K + q^m M} \\
\int \theta_h g_h(\eta) d\eta + \theta_f \eta_f + \theta_b \eta_b &= \vartheta \\
\theta^n_f \eta_f + \int \theta^n_h g_h(\eta) d\eta &= 0 \\
\int \theta^d_h g_h(\eta) d\eta + \theta^d_b a_b &= 0 \\
\theta^m_f \eta_f &= 1 - \vartheta
\end{aligned}
$$

where $\vartheta = q^k K/(q^k K + q^m M)$. *The long term assets prices are only implicitly defined by the* *asset pricing equations and so must satisfy consistency with Itô's Lemma for $l \in \{k, n, m\}$:*

$$\begin{aligned}\mu_{q^l} q^l(\boldsymbol{S}) &= (D_x q^l(\boldsymbol{S}))^T \boldsymbol{\mu}_s + \frac{1}{2} tr \Big\{ (\boldsymbol{\sigma}_s(\boldsymbol{S}, \boldsymbol{\theta}_h) \odot \boldsymbol{S})^T (\boldsymbol{\sigma}_s(\boldsymbol{S}, \boldsymbol{\theta}_h) \odot \boldsymbol{s}) D_s^2 q^l(\boldsymbol{S}) \Big\} \\ &\quad + \mathcal{L}_g q^l(\boldsymbol{S}) \\ \boldsymbol{\sigma}_{q^l} q^l(\boldsymbol{S}) &= (\boldsymbol{\sigma}_s \odot \boldsymbol{S})^T (D_s q^l(\boldsymbol{S}))\end{aligned}$$

Proof. See Appendix A. □

Block 3 implicitly pins down both (i) equilibrium asset return by market clearing conditions and (ii) asset price level (separate set of partial differential equations) in the economy. Asset market clearing conditions equate aggregate positions and supplies, so together with the FOCs in Block 1 they pin down the vector of equilibrium *risk premia* (i.e., return gaps across assets) that is consistent with the aggregation of portfolio. In per-wealth units, the resource constraint combined with the Euler equation pins down the risk-free rate; equivalently, given a target consumption-to-wealth ratio it determines the level of total wealth. Because long-lived prices q^l are state-dependent functions of $\boldsymbol{S} = (\boldsymbol{s}, g_h)$, their drifts and diffusions must satisfy the Itô-consistency PDEs in Theorem 3. The coefficients depend on the distributional block via (η_b, η_f, g_h) and the operator $\mathcal{L}_g$, so price dynamics are endogenously linked to the cross-sectional evolution.

2.4 Comparison to Other Models

This system of equations is difficult to solve because, unlike in most models, all three blocks are non-trivial. To understand why this is the case, it is instructive to compare our model to other macro-finance models.

(i). For a representative agent model, block 2 is not applicable because there is no distribution and block 3 is less complicated because the goods market condition simply becomes $c + (\iota - \phi(\iota))K = y$, which can be substituted into equations in block 1. In this case, the set of equations can be simplified to a differential equation for q. Even for models with a continuum of agents, many researchers follow the approach in Krusell and Smith (1998) and approximate the distribution by the first moment and so eliminate the need to track the full distribution.

(ii). For the continuous time version of Krusell and Smith (1998) discussed in Gu et al. (2023), we have a distribution of agents so block 2 is non-trivial. However, this model has no long-term assets and so we can derive closed form expressions for all prices in term of the distribution. This implies that block 3 can be trivially satisfied and we can combine all equilibrium conditions into one "master" partial differential equation.

(iii). For models such as Basak and Cuoco (1998) and Brunnermeier and Sannikov (2014) discussed in Gopalakrishna (2021), the HJBE can be solved partially in closed form so that we can get an analytical expression for the dependence of the value function on idiosyncratic wealth. This means that block 1 can be reduced into scaled PDE and substituted into the block 3.

3 Computational Methodology and Algorithm

In this section, we outline our algorithm for solving the model. Conceptually, we can view our approach as a type of "projection" onto a neural network. At a high level, this involves:

(a) Replacing the agent continuum by a finite dimensional distribution approximation,

(b) Representing the equilibrium functions by neural networks with the states as inputs,

(c) Training the neural network parameters to minimize the loss in the equilibrium conditions on randomly sampled points from the state space.

Although this approach is straightforward to describe at a high level, implementing it successfully involves many non-trivial decisions that we discuss in this section.

3.1 Finite dimensional distribution approximation

Conceptually, the finite dimensional approximation approach replaces the household distribution state by a finite collection of $I < \infty$ price taking agents. A natural and frequently raised concern with this approach is that the simulation of the I agent economy would contain idiosyncratic noise and so be inconsistent with perceived law of motion. However, there are a number of reasons why this is not a problem in our algorithm. First, we do not use simulation to solve the model because we are working with a continuous time analytical formulation of the problem. So, concerns about simulation accuracy are unrelated to the accuracy of the neural network solution. Second, we solve for an equilibrium in which agents behave as price takers and forecast prices under the assumption that the idiosyncratic death shocks have averaged out and so perceived the law of motions do not contain idiosyncratic risk. Third, when we do need to simulate the solved model (e.g. to generate time paths or impulse responses), we use our neural network solution to approximate a finite difference approximation to the KFE and so are able to simulate the limiting economy with a continuum of agents. We do this following the approach we developed in Gu et al. (2023) and summarized in Appendix C to this paper. In this sense, we exploit the continuous-time analytical formulation to be able to maintain the convenience of a finite agent economy without have to deal with the finite sample noise problem that appears in discrete-time simulation based training methods.

3.2 Neural network representation and loss function

A "direct" implementation of our deep learning approach would be to parameterize all the equilibrium objects and then train a large collection of neural networks to minimize a large loss function that combines all the general equilibrium equations described in Theorem 1. Although this should work in principle, it is difficult to implement in practice. Instead, we rewrite the equilibrium characterization to "help" the deep learning algorithm to train the neural networks.

First, we approximate the equilibrium functions rather than the partial equilibrium functions. Under the finite agent approximation, the aggregate state space is $\hat{\boldsymbol{S}} := (z, K, \eta_1, \ldots, \eta_I, \eta_b, \eta_f) \in \mathcal{S}$. In equilibrium, all the functions can be expressed directly in terms of the aggregate state $\hat{\boldsymbol{S}}$. For example, the function $\xi_h(a_i, \hat{\boldsymbol{S}})$ has an equilibrium representation given by:

$$\Xi_h(\hat{\boldsymbol{S}}) := \xi_h\left(\eta_i A\left(\hat{\boldsymbol{S}}\right), \hat{\boldsymbol{S}}\right)$$

where $A(\hat{\boldsymbol{S}}) = q^k(\hat{\boldsymbol{S}})K + q^m(\hat{\boldsymbol{S}})M$ is equilibrium aggregate wealth. We solve directly for the equilibrium functions (i.e. Ξ_h) rather than for the partial equilibrium functions (i.e. ξ_h) in order to avoid having to nest the neural network approximation for prices (i.e. q^k, q^m) inside the neural network approximation for other other variables when we impose equilibrium.

Second, we use Neural Nets to represent variables that are relatively easy to train. This leads us to parameterize the following variables by Neural Nets:

$$\begin{aligned}
\hat{\omega}_h &: \mathcal{S} \to \mathbb{R},\ (\hat{\boldsymbol{S}}, \Theta_{\omega_h}) \mapsto \hat{\omega}_h(\hat{\boldsymbol{S}}; \Theta_{\omega_h}),\\
\hat{\Omega}_h &: \mathcal{S} \to \mathbb{R},\ (\hat{\boldsymbol{S}}, \Theta_{\Omega_h}) \mapsto \hat{\Omega}_h(\hat{\boldsymbol{S}}; \Theta_{\Omega_h}),\\
\hat{\theta}^l_i &: \mathcal{S} \to \mathbb{R},\ (\hat{\boldsymbol{S}}, \Theta_{\theta_j}) \mapsto \hat{\boldsymbol{\theta}}_j(\hat{\boldsymbol{S}}; \Theta_{\theta_j}), \quad \forall l \in \{k, n, m\}, i \in \{h, f, b\}\\
\hat{q}^l &: \mathcal{S} \to \mathbb{R},\ (\hat{\boldsymbol{S}}, \Theta_{q^l}) \mapsto \hat{q}^l(\hat{\boldsymbol{S}}; \Theta_{q^l}), \quad \forall l \in \{n, m\}\\
\hat{\mu}_{q^l} &: \mathcal{S} \to \mathbb{R},\ (\hat{\boldsymbol{S}}, \Theta_{\mu,q^l}) \mapsto \hat{\mu}_{q^l}(\hat{\boldsymbol{S}}; \Theta_{\mu,q^l}), \quad \forall l \in \{k, n, m\}\\
\hat{\boldsymbol{\sigma}}_{q^l} &: \mathcal{S} \to \mathbb{R},\ (\hat{\boldsymbol{S}}, \Theta_{\sigma,q^l}) \mapsto \hat{\boldsymbol{\sigma}}_{q^l}(\hat{\boldsymbol{S}}; \Theta_{\sigma,q^l}), \quad l \in \{k, n, m\}
\end{aligned}$$

where $\omega := c/a$ denotes the household consumption-to-wealth ratio during their lifetime, $\Omega := \mathcal{C}/a$ denotes the household consumption-to-wealth ratio at death, and Θ_ν denotes the parameters for the Neural Net approximation of variable ν. Why do we approximate these variables? In general, it is easier for the Neural Net to approximate well behaved, bounded functions. This guides our choices about how to parametrize the household optimization variables. It is easier to approximate $\xi_h = \partial_a V_h$ than V_h because it is easier to impose concavity. It is even easier to approximate the consumption-to-wealth ratio $\omega_h(\eta_i)$ and then reconstruct $\xi_h(\eta_i) = (\omega_h(\eta_i)\eta_i A)^{-\gamma}$ because then the explosive curvature is encoded analytically.

Third, where possible, we impose market clearing explicitly rather than including the market clearing conditions as part of the loss function. Given the neural network approximations $(\hat{\omega}_h, \hat{\Omega}_h, \hat{\boldsymbol{\theta}}_j, \hat{q}^l, \hat{\mu}_{q^k}, \boldsymbol{\sigma}_{q^l})$, we can solve for the other equilibrium variables explicitly using linear algebra. The neural network approximations then need to satisfy the following equations (after imposing market clearing and with $\hat{\Xi} = u'(\hat{\omega}(\hat{\boldsymbol{S}})\eta\hat{q}^k(\hat{\boldsymbol{S}})K)$):

$$
\begin{aligned}
\mathcal{L}_\omega(\hat{\boldsymbol{S}}) &= (r^d - \tau_h - \rho_h - \lambda_h)\hat{\Xi} + \mu_\Xi(\hat{\boldsymbol{S}}) + \psi_{h,k}(\theta_h^k(\hat{\boldsymbol{S}})) \\
&\quad - \partial_{\theta_h^k}\psi_{h,k}(\theta_h^k)\theta_h^k(\hat{\boldsymbol{S}}) + \psi_{h,n}(\theta_h^n(\hat{\boldsymbol{S}})) - \partial_{\theta_h^n}\psi_{n,k}(\theta_h^n)\theta_h^n(\hat{\boldsymbol{S}}) && \ldots\text{Euler eq.} \\
\mathcal{L}_\Omega(\hat{\boldsymbol{S}}) &= \hat{\Omega} - \eta A(\hat{\boldsymbol{S}})\mathcal{W}(\theta_h^k(\hat{\boldsymbol{S}}), \theta_h^n(\hat{\boldsymbol{S}})) && \ldots\text{Death cons.} \\
\mathcal{L}_{\theta_h^l}(\hat{\boldsymbol{S}}) &= r^l - r^d + \lambda\partial_{\theta_h^l}\mathcal{W}(\theta_h^k, \theta_h^n)\frac{\mathcal{U}'(\mathcal{C})}{a\xi_h} + \partial_{\theta_h^l}\psi_{h,l} + \sigma_{\xi_h}\sigma_{q^l}, \quad l \in \{k, n\} && \ldots\text{FOC hh.} \\
\mathcal{L}_{\theta_f^l}(\hat{\boldsymbol{S}}) &= r^l - r_f^n + \sigma_{\xi_f}(\sigma_{q^l} - \sigma_{q^n}), \quad l \in \{k, m\} && \ldots\text{FOC fund.} \\
\mathcal{L}_{\theta_b^l}(\hat{\boldsymbol{S}}) &= r^l - r_f^d + \sigma_{\xi_b}(\sigma_{q^l} - \sigma_{q^n}), \quad l \in \{k, m\} && \ldots\text{FOC bank.} \\
\mathcal{L}_{\mu_{q^l}}(\hat{\boldsymbol{S}}) &= (D_{\hat{\boldsymbol{S}}}q^l)^T\boldsymbol{\mu}_{\hat{\boldsymbol{S}}} + \frac{1}{2}\text{tr}\left\{(\boldsymbol{\sigma}_{\hat{\boldsymbol{S}}}(\hat{\boldsymbol{S}}, \boldsymbol{\theta}_h) \odot \hat{\boldsymbol{S}})^T(\boldsymbol{\sigma}_x(\hat{\boldsymbol{S}}, \boldsymbol{\theta}_h) \odot \hat{\boldsymbol{S}})D^2_{\hat{\boldsymbol{S}}}q^l\right\} && \ldots\text{Consistency} \\
\mathcal{L}_\sigma(\hat{\boldsymbol{S}}) &= \hat{\boldsymbol{\sigma}}_q(\hat{\boldsymbol{S}}) - (\boldsymbol{\sigma}_{\hat{\boldsymbol{S}}} \odot \hat{\boldsymbol{S}})^T(D_{\hat{\boldsymbol{S}}}q^l), \quad \forall l \in (k, n, m) && \ldots\text{Consistency}
\end{aligned}
\tag{3.1}
$$

3.3 Algorithm

We outline the steps in Algorithm 1 below. Given the current guesses of the neural networks, we could express the loss function (3.1) directly by elementary algebras of (i) neural network approximated variables and (ii) derivatives of the neural network approximated variables by automatic differentiation. We then update our guesses for the neural network approximations.

Each neural network is a fully-connected feed-forward type and has 2 hidden layers and 256 neurons in each layer. We train using an ADAM optimizer with a learning rate scheduler for 50k iterations. Figure 5 presents the L-2 loss from the quantitative model over iterations.

The loss decreases over time, although not monotonically due to the stochastic nature of the learning process. After 50,000 iterations, the average Euler equation loss is 8.5×10^{-5} in marginal utility units. To test the efficacy of our numerical algorithm, we present three testable models from the macro-finance literature in the Online Appendix.

Algorithm 1: Pseudo Code

1: Initialize neural network objects ($\hat{\omega}_h$, $\hat{\Omega}_h$, $\hat{\boldsymbol{\theta}}_j$, $\hat{q}^l$, $\hat{\mu}_{q^k}$, $\boldsymbol{\sigma}_{q^l}$) with parameters $\boldsymbol{\Theta}$,
2: Initialize optimizer.
3: **while** Loss > tolerance **do**
4: Sample N new training points: $\left(\hat{\boldsymbol{S}}^n = \left(z^n, \zeta^n, K^n, (\eta_i)^n_{i \leq I}, \eta^n_b, \eta^n_f\right)\right)^N_{n=1}$.
5: Calculate equilibrium at each training point $\hat{\boldsymbol{S}}^n$ given the current guesses for neural network objects ($\hat{\omega}_h$, $\hat{\Omega}_h$, $\hat{\boldsymbol{\theta}}_j$, $\hat{q}^l$, $\hat{\mu}_{q^k}$, $\boldsymbol{\sigma}_{q^l}$).
5: Construct the loss as:

$$\hat{\mathcal{L}}(\hat{\boldsymbol{S}}^n) = (\mathcal{L}_\omega + \mathcal{L}_\Omega + \mathcal{L}_{\theta^l_h} + \mathcal{L}_{\theta^l_f} + \mathcal{L}_{\theta^l_b} + \mathcal{L}_{\mu_{q^k}} + \mathcal{L}_\sigma)(\hat{\boldsymbol{S}}^n; \boldsymbol{\Theta})$$

where $\hat{\mathcal{L}}_v$ is defined by equation (3.1) for each variable v.
6: Update $\boldsymbol{\Theta}$ using stochastic gradient descent.
7: **end while**

4 Calibration

We calibrate the model using parameter values from literature whenever possible, and target moments for the remaining parameters. The calibration period spans 2010Q1-2025Q2 so we interpret our model as indirectly estimating the Basel III regulatory parameters. Table (1) reports the full set of parameters and the set of targeted moments. We classify the calibration targets into three groups — (i) macroeconomic, (ii) asset pricing, and (iii) cross-sectional moments.

Macroeconomic parameters: The mean-reversion of TFP is set to 0.3, following Gertler et al. (2019), and the volatility of TFP is set to 0.10 to target a 3.5% output growth volatility. The depreciation rate is chosen to match an annualized output growth rate of 2.6%, which is consistent with the real long-run output growth rate used in the literature. The investment friction parameter is calibrated to match the volatility of the private investment-to-capital ratio. The model successfully generates an investment-to-capital ratio of 11.8%, close to the data, even though untargeted in the calibration.

Asset pricing parameters: We set the household risk aversion parameter to 1, following Krishnamurthy and Li (2020), and discount rates to 0.05, consistent with the literature

Targeted moments	Parameter	Value	Target moment (Data value)	Target
TFP mean reversion	β_z	0.30	Literature	-
TFP volatility	σ_z	0.10	Output growth vol = 0.034	
Depreciation	δ	0	Output growth =0.025	0.0263
Investment friction	κ	95	Investment vol =0.076	0.086
Household risk aversion	γ, Γ	1	Literature	-
Bank risk aversion	γ_b	0.85	Capital Sharpe Ratio = 1.44	1.64
Fund risk aversion	γ_f	0.10	Annuity return = 0.035	0.033
Discount rate (hh.)	ρ_h	0.05	Literature	-
Discount rate (fund)	ρ_e	0.05	Literature	-
Discount rate (bank)	ρ_b	0.05	Literature	-
Capital constraint	$\bar{\psi}_k$	1e-5	Median household capital share =0.40	0.42
Death shock intensity (hh.)	λ_h	0.10	Average life =35	10
Death shock intensity (fund)	λ_f	0.20	Equity recapitalization	5yrs
Death shock intensity (bank)	λ_b	0.20	Equity recapitalization	5yrs
Transfer weight (hh.)	ϕ_h	0.03	Median hh. annuity share = 0.37	0.40
Transfer weight (fund)	ϕ_f	0.16	Fund A/E =1.40	1.45
Transfer weight (bank)	ϕ_b	0.10	Bank A/E =1.50	1.53
Bond maturity	λ_m	0.033	Maturity of LT bonds	30 yrs
Untargeted moments			Data	Model
Risk premium - shadow (%)			8.5	7.3
Term premium (%)			0.7	0.8
Investment/capital rate (%)			14.0	11.8

Table 1: List of model parameters and calibration targets. All values are annualized. The time period is from 2010 Q1 to 2025Q2.

(e.g., Gertler et al. (2019)). The bank risk aversion is set to 0.85 to target a capital Sharpe ratio of 1.44, computed by estimating the risk premium using a factor model. Specifically, we regress equity market returns on dividend yield and estimate the Sharpe ratio from the fitted values. The fund risk aversion is chosen to target an average annuity return of 3.5%.[3] The household death intensity reflects the average retirement period in the population and is set to 0.1. The death intensity of intermediaries is set to 0.20, motivated by their average equity recapitalization duration. Black, Floros and Sengupta (2016) reports that between 2001 and 2014, around 30% of the publicly listed banks (BHCs) in the US raised equity. We are not aware of comparable statistics for the fund sector and therefore assume the same number. The transfer weights of households, the fund, and the bank are chosen to match the respective leverage ratios. The household transfer weight is calibrated to match the ratio of risky assets to total wealth for the median household in the Survey of Consumer Finance (SCF) data. Bank leverage in the data is around 5 (Krishnamurthy and Li (2020), while firms' leverage is much lower (around 1.3 from COMPUSTAT). Since our "bank" combines both financial and non-financial institutions that hold risky capital, we target a conservative leverage ratio of 1.5.[4] For the pension fund sector, the leverage ratio is around 1.4, closer to the data.[5] We set bond maturity to 30 years to represent a long-duration bond. Finally, we set the death tax rate to 0% for simplicity, but our results are robust to a 17% rate that reflects the average estate tax rate after exemptions according to the CBO and IRS-SOI data.[6] The intermediary portfolio penalty parameters $\psi_b^k, \psi_f^k, \bar{\theta}_b^k, \bar{\theta}_b^k$ are set according to Table 4 in the baseline model and will be varied in counterfactual experiments. We assume no penalty on bond holdings ($\psi_b^m = 0, \psi_f^m = 0$). We set $\beta = 0.5$ so that flow and terminal utility carry the same weight. We pick the smallest value of deposit penalty ($\bar{\psi}_d = 2.0$) that prevents shorting of household capital. In the baseline model, we assume no annuity penalty (i.e., $\bar{\psi}_n$=0) and use it in the counterfactual experiments.

The untargeted asset pricing moments generated by the model are close to the data. The model produces a shadow capital risk premium of 7.3%, and a term premium of 0.8%, reasonably close to the empirical values. The shadow risk premium is computed as the difference between the expected capital return and the shadow risk-free rate implied by the

[3] Annuity returns are difficult to compute and lack consensus. We rely on Mitchell, Poterba, Warshawsky and Brown (1999) to obtain a conservative estimate of 3.5% net of fees.

[4] Since the year 2010, non-financial corporate sector assets have been around \$45 trillion USD, of which \$30 trillion are equity. Banking sector assets have been around \$30 trillion (net of reserves and Treasuries), of which \$2.57 trillion are equity. The combined sector implies a leverage ratio of 1.77 which is closer to our target.

[5] Source: FRED database. We use 'BOGZ1FL594090005Q' for total pension fund assets, and 'BOGZ1FL574190005Q' for liabilities.

[6] Source: Office (2017) and Internal Revenue Service, Statistics of Income Division (2023).

Euler equation without participation constraints.[7] The model also directionally matches the beta of the fund's equity exposure to capital return, even though the betas are not directly targeted. Table (2) reports the factor regression results where the fund equity returns are proxied by changes in the fund wealth share in the model. The results are consistent with Koijen and Yogo (2022), who show that the variable annuity insurers' stock returns have a positive beta with respect to stock and a negative beta with respect to 10-year Treasury bond returns. While the interest rate is endogenous in our model, the quantitative exercise indicates that an unexpected increase in the rate does decrease the fund's wealth, in line with Koijen and Yogo (2022).

Factor	Data (1999-2017)	Data (2010-2017)	Model
Stock market return	1.36	1.11	0.82
	(0.19)	(0.08)	(0.03)
Long term bond return	-0.01	-1.28	-0.12
	(0.32)	(0.43)	(0.04)
Observations	228	96	249

Table 2: Risk exposure of fund sector. The table reports betas from a factor regression of fund equity returns on stock returns and long-term bond returns. Data values are taken from Koijen and Yogo (2022), and corresponds to the period 2010-2017. Baseline refers to the economy where fund is allowed to hold capital. Regulated refers to the economy where the fund is shut out of the capital market, and holds only government bonds. Heteroskedasticity adjusted standard errors are given in parenthesis.

Cross-sectional moments: Lastly, our model generates rich cross-sectional moments that are broadly consistent with the data, even though they are not explicitly targeted. We set the household capital constraint parameter ψ_h to match the risky asset holdings of the median household in the SCF data, and then evaluate how well the model replicates moments across the distribution.[8] Figure (1) shows households' risky capital, annuity, and risk-free asset shares as a fraction of total wealth in both the data and the model. We can see that the model does a good job of matching the large blocks in the distribution at the 25th, 50th, and 75th percentiles. We also assess the model's performance in matching the response of household wealth to negative TFP shocks. Empirically, we measure changes in the wealth distribution following shocks to the net worth of U.S. insurance funds. Shocks are estimated as innovations in the autoregression $\hat{a}_t = \beta_0 + \beta_1 \hat{a}_{t-1} + u_t$, normalized by lagged equity value $\hat{f} := \frac{u_t}{\hat{a}_{t-1}}$. We then apply local projections in the spirit of Jordà (2005), regressing shocks

[7]The shadow risk free rate $\bar{r}^d_t$ is computed as $\bar{r}^d_t = \tau_{h,t} + \rho_h + \lambda_h - \mu^h_{\xi,t}$.

[8]We remove households who have short portfolio positions to be consistent with the SCF data.

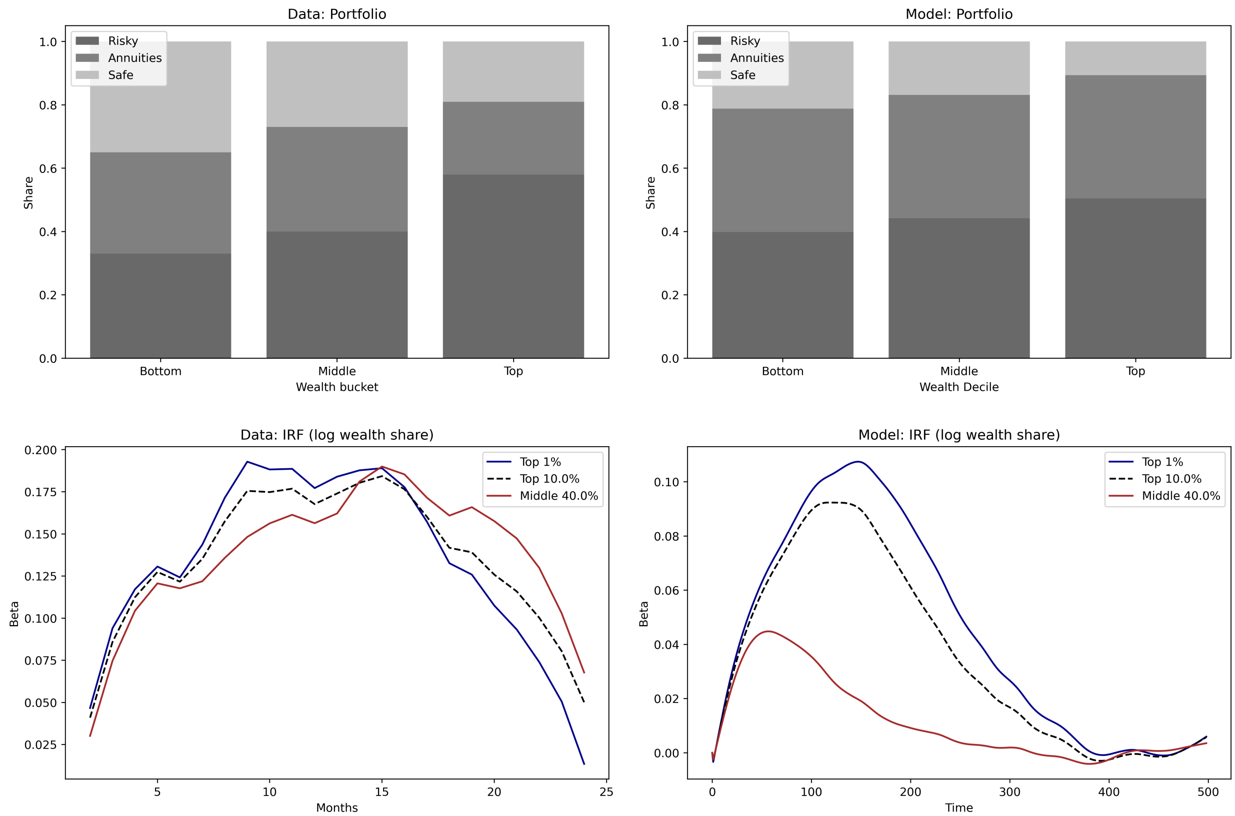

Figure 1: The top row figures present the portfolio holdings of households across 25th (Bottom), median (Middle), and 75th (Top) percentiles from the SCF data and model, respectively. The bottom left figure plots the impulse response of wealth distribution to risk premium ($\beta_{p,h}$) obtained from the regression $\log\left(W_{p,t+h}/W_{p,t}\right) = \alpha_{p,h} + \beta_{p,h}\hat{f}_t + \epsilon_{p,t+h}$. The data for wealth percentiles come from Saez and Zucman (2016), and risk premium is estimated using a factor model. The bottom right figure plots the impulse response of wealth share of households at different percentiles to a 2 std. deviation negative TFP shock.

to fund net worth on the wealth share of households at different percentiles. Specifically, we run the following regression

$$\log\left(\frac{W_{p,t+h}}{W_{p,t}}\right) = \alpha_{p,h} + \beta_{p,h}\hat{f}_t + \epsilon_{p,t+h}$$

for horizons $h = 1$ to 20 quarters where $w_{p,t+h}$ denotes household wealth at percentile p at horizon h. We repeat this regression for $p \in \{1.0, 10.0, 40.0\}$, corresponding to the top 1%, top 10%, and middle 40% of the wealth distribution. The household wealth distribution is taken from Saez and Zucman (2016), and the fund wealth share series is constructed from the Financial Accounts of the United States (FRB) following Koijen and Yogo (2021). The empirical evidence shows that disruptions to the insurance sector's wealth raise the wealth share of the top percentile households, while the bottom 50% experience little change.[9] Our model captures the qualitative pattern, although the quantitative fit is limited, since our proxy for fund wealth share does not perfectly correspond to fund equity returns in the data.

5 Counterfactual: Revisiting Basel III and IV

In this section, we use our calibrated model to study the macroeconomic impact of changes to the current Basel III regulatory system. Previous macro-finance work has focused on the high level regulatory tradeoff between growth and stability. Our model allows us to extend this analysis to consider the heterogeneous impact of regulation across different financial intermediaries and households.

In Section 4, we calibrated our baseline economy over 2010Q1-2024Q4, a period when financial institutions operated under tighter regulatory oversight in the aftermath of the global financial crisis. Pension and insurance funds were subject to risk-based solvency and liability-oriented rules, which granted capital relief for duration matching of long-term assets and liabilities. Banks, by contrast, faced binding leverage requirements under Basel III that capped the size of their balance sheets relative to equity, regardless of asset maturity. As banks deleveraged, non-bank financial institutions - including pensions and insurers - absorbed a growing share of long-duration risky assets, reallocating toward long-term corporate bonds, private credit, and alternatives (Koijen and Yogo (2022), Begenau, Liang and Siriwardane (2024)). This shift was reinforced by the decline in interest rates, which raised the present value of liabilities and incentivized funds to pursue higher-yielding, long-duration investments. The reduction in interest rates increased their liabilities, incentivizing them to

[9] We do not plot the bottom 50% as its response is not statistically different from zero.

tilt towards long-term assets.

We use this environment to study two counterfactual regulatory regimes. In the first, we impose a bank-style leverage restriction on the fund sector by decreasing the parameter $\bar{\theta}_f^k$ that captures the maximum capital holdings the fund can have without incurring a penalty. This "fund" economy eliminates duration-matching credits and directly caps total exposure to risky capital and bonds. In the second, we tighten the leverage requirement on banks by increasing the parameter ψ_b that captures the strength of the leverage constraint penalty. This "bank" economy reflects concerns from critics that even after Basel III, banks remain excessively leveraged and under-capitalized (Admati and Hellwig (2013), Acharya, Engle and Pierret (2014)). Together, these counterfactuals allow us to quantify how extending or strengthening leverage constraints across institutions would affect asset prices and the distribution of household wealth. We summarize the regulatory parameters in Table (4).

	Baseline	Counterfactual: Fund-regulated	Counterfactual: Bank-regulated
Bank regulation parameters			
ψ_b^k	0.1	0.1	0.15
ψ_b^m	2.0	2.0	2.0
$\bar{\theta}_b^k$	1.0	1.0	1.0
$\bar{\theta}_b^m$	5.0	5.0	5.0
Fund regulation parameters			
ψ_f^k	0.1	0.1	0.1
ψ_f^m	2.0	2.0	2.0
$\bar{\theta}_f^k$	10.0	1.0	10.0
$\bar{\theta}_f^m$	5.0	5.0	5.0

Table 3: Regulatory parameters across different regulatory regimes.

We summarize the key macroeconomic statistics from the different counterfactual experiments in Table 4 below. The economics behind these results is complicated. So, to build intuition, we discuss the results progressively. We start in Subsection 5.1 by examining the macroeconomic impact of the different regulatory regimes at the sector level. Then, in Subsection 5.2, we examine the distributional consequences among households. Finally, in Subsection 5.3, we bring everything together and discuss how the government faces tradeoffs between growth, stability, and inequality.

	Baseline	Counterfactual: Fund-regulated	Counterfactual: Bank-regulated
Price results			
Sharpe Ratio	1.649	5.452	1.719
Term Premium (%)	0.785	1.307	1.722
Conv. Yield (%)	0.275	0.931	-0.479
Govt. bond price	0.220	0.220	0.213
Annuity spread (%)	-1.106	-0.985	-0.101
Aggregate results			
Output (%)	2.633	2.299	2.310
Investment (%)	11.785	8.299	8.400
Total consumption (hh.)	0.704	0.788	0.614
Sector level results			
Fund A/E	1.454	1.081	2.091
Bank A/E	1.536	1.312	1.362
Wealth (hh.)	1.640	1.587	1.395
Cons. Risk (hh.) (%)	4.196	-0.106	2.790
Wealth share Risk (hh.) (%)	-0.013	-0.0007	-0.015
Household distributional results (hh.)			
C/W (Top 1%/Median)	1.356	2.006	1.354
Wealth (Top 1%/Median)	1.443	2.193	2.059
Cons. Risk (Top 1%/Median)	1.035	-2.843	1.101
Wealth share Risk (Top 1%/Median)	0.630	0.660	0.693
Gini Coefficient	0.156	0.235	0.222

Table 4: Equilibrium across different regulatory regimes.

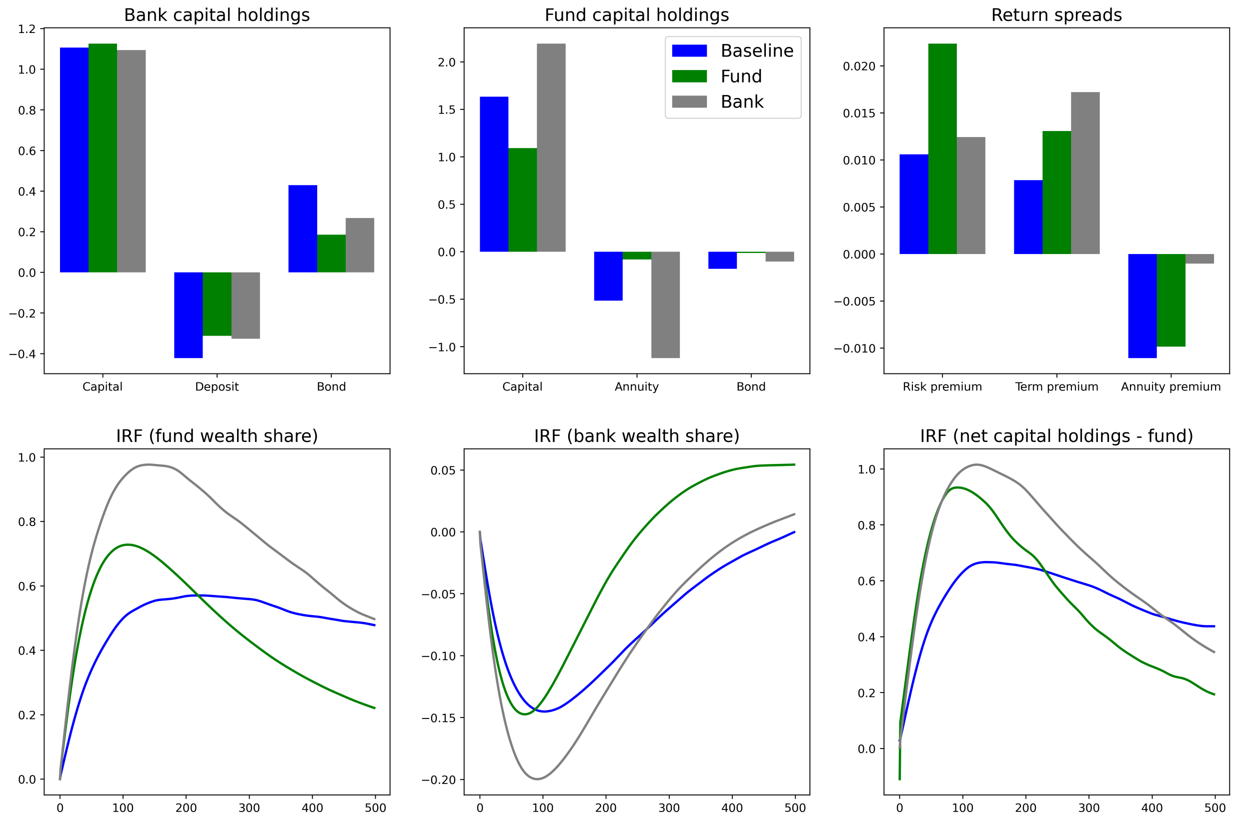

Figure 2: Sector level: The top left and center panel presents the bank and fund capital holdings across three economies, respectively. The top right figure presents the spreads. The bottom left and center panel figures present the impulse response of wealth share of fund, bank, and median household to a 2 std. deviation negative TFP shock. The bottom right panel figures trace out the portfolio returns of fund net of bank.

5.1 Sector Level Results

We begin by studying how regulation affects the financial sector before turning to households. Broadly, we observe that regulation determines (i) which agent, and to what extent the agent acts as a "back-stop" during bad times, and (ii) the magnitude of return spreads in the risky assets. Figure 2 shows the ergodic mean portfolio holdings of the fund and the bank, mean return spreads on the risky assets, and impulse responses of sectoral wealth shares to a two-standard deviation negative TFP shock in the baseline and counterfactual economies.

In the baseline, funds act as shock absorbers: during downturns, they increase their capital holdings relative to banks, stabilizing the capital prices but charging a high annuity price. As a result, fund wealth share raises, while bank share declines. This behaviour reflects differences in the liability structures: fund liabilities are long-term that fall in value during TFP shocks, while the bank liabilities are short-term and are unaffected. Hence, funds are better positioned to absorb risk, but at the cost of charging high annuity prices lowering household wealth.

The extent to which funds tax households through annuity premiums to absorb risk changes with regulation. Table 4 summarizes sector-level macroeconomic and asset pricing moments across regimes in the top panel. In the fund-regulated economy, funds contract their balance sheet by holding less capital and supplying less annuity. The aggregate capital holding from the financial sector falls, pushing up the capital return spread. The household sector responds by substituting away from annuities and into risky capital. Lower capital prices depress aggregate output and investments but also lower consumption and wealth share risk of households since low financial sector leverage leads to low endogenous price volatility. This highlights a central trade-off: tighter regulation stabilizes household risk exposures but at the expense of macroeconomic outcomes. In the bank-regulated economy, banks shrink their balance sheets by reducing deposits and capital holdings. Funds expand instead, issuing more annuities at attractive terms and thereby increasing their absorbing capacity. This shift raises fund capital holdings and wealth shares in response to shocks. The macroeconomic and distributional trade-offs are similar to those in the fund-regulated economy, although quantitatively less pronounced.

5.2 Distributional implications

An important feature of the model is the ability to characterize the general equilibrium relationship between participation constraints, inequality, and asset price dynamics. In this subsection, we explore these connections. The difference between the drift of the wealth share of any two households i and j can be expressed as:

$$\mu_{\eta_j,t} - \mu_{\eta_i,t} = \underbrace{(\theta^k_{j,t} - \theta^k_{i,t})(r^k_t - r^d_t - \boldsymbol{\sigma}^k_{q,t} \cdot \boldsymbol{\sigma}^k_{q,t})}_{=:(\mu_{\eta_j,t}-\mu_{\eta_i,t})^K} + \underbrace{(\theta^n_{j,t} - \theta^n_{i,t})(r^n_t - r^d_t - \boldsymbol{\sigma}^k_{q,t} \cdot \boldsymbol{\sigma}^n_{q,t})}_{=:(\mu_{\eta_j,t}-\mu_{\eta_i,t})^N}$$
$$- (\omega_j - \omega_i) + \lambda_h \phi_h \left(\frac{1}{\eta_{j,t}} - \frac{1}{\eta_{i,t}} \right) \tag{5.1}$$

The first term in (5.1) captures how participation constraints and risk aversion impact the excess return that different agents can earn. When $\eta_{j,t} > \eta_{i,t}$ is higher, then agent j holds more wealth in capital and so gains wealth share compared to the poorer agents who are unwilling to pay the cost to participate in the capital market. This has sometimes been referred to as the "scaling" effect in the literature—wealthier agents have access to better investment opportunities and so gain wealth more quickly. The second term in (5.1) captures the impact of risk exposure on the average wealth drift. Agents holding more capital are also more exposed to aggregate risk in the economy. This additional impact of scaling up into risky investment opportunities that is not present in macroeconomic inequality models without aggregate risk. The third term in (5.1) captures the impact of the death rate in the economy. This is the main force that stabilizes the wealth distribution in the economy. Other models have attributed this to many possible features (e.g. new entrants with better skills, idiosyncratic risk, etc.). We have little to say about it in our model and so simply allocate it to a death rate. The final term in (5.1) captures how a lower marginal propensity to consume out of wealth, $\omega_j < \omega_i$, leads to greater wealth accumulation.

Figure 3 reports household capital allocation, impulse responses to a two-standard deviation negative TFP shock, and decomposition of wealth share drift across percentiles. In the baseline economy, substantial heterogeneity in capital holdings emerges from participation constraints: wealthier households hold more capital due to easy access to capital markets, while annuity holdings remain similar across the distribution due to the "preferred-habitat" nature of annuity demand. In response to a shock, households that have a higher risk exposure lose wealth initially, before recovering. The decomposition result in the bottom panel reveals that portfolio return differences contribute significantly to the difference in the wealth share drift between the top 1% and top 10% households. This "scaling effect" - where wealthier households access better investment opportunities - reinforces tail inequality. Because capital return spikes during recessions, households with greater risk exposure eventually gain wealth share, generating a fat-tailed distribution and procyclical inequality dynamics.

Regulation amplifies these effects through its effect on asset prices. Relative to the baseline, both the fund and the bank regulated economies exhibit a larger difference in capital

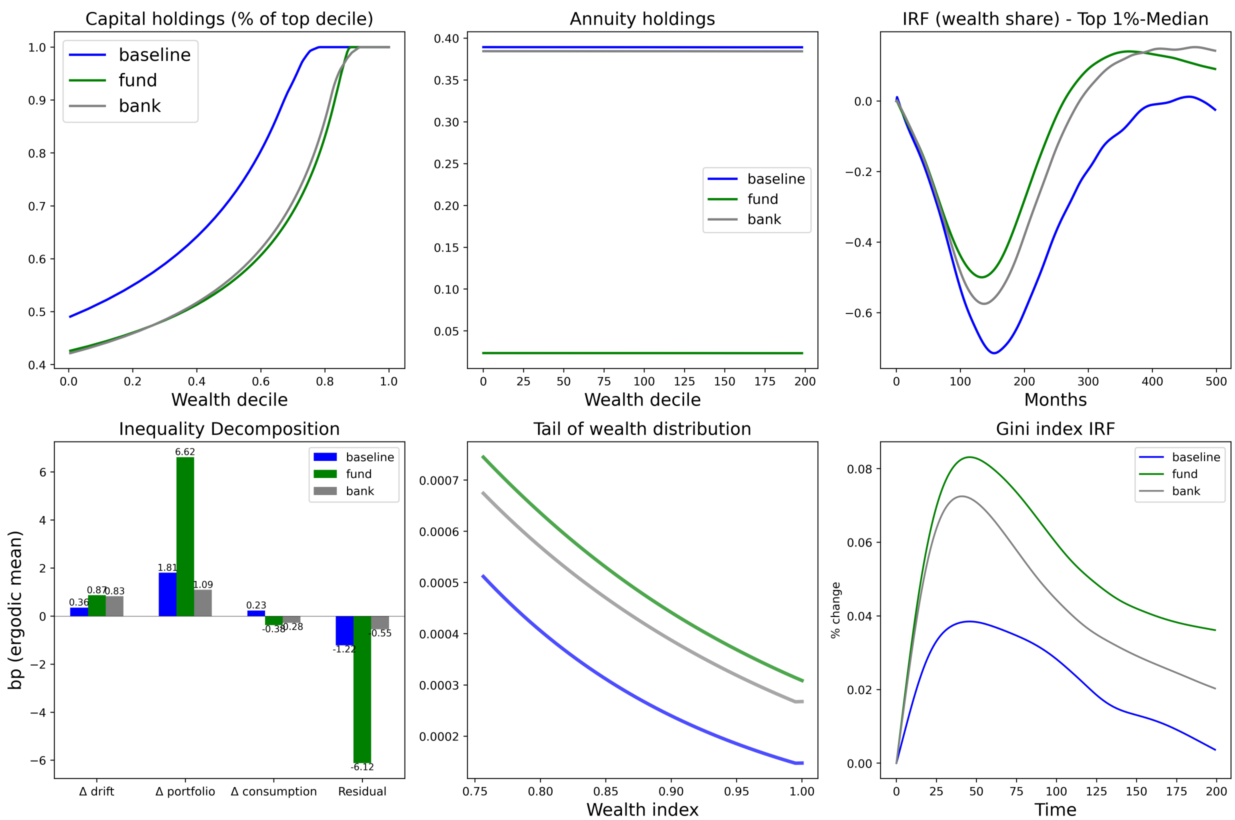

Figure 3: Distributional outcomes: The top left panel presents the capital holdings of households relative to the top wealth decile in the baseline, fund-regulated, and bank-regulated economy. The top center panel presents the level of annuity holdings. The top right figure presents the impulse response of top 1% wealth share of households relative to median to a 2 s.d. negative TFP shock. The bottom left panel presents the decomposition of difference in wealth share drift between 99-th pctl. and 90-th pctl. household. The bottom center panel presents the tail of wealth distribution, and the bottom right panel presents the impulse response of Gini coefficient to a 2 s.d. negative TFP shock. In all plots, the blue line corresponds to baseline economy, green line corresponds to fund restricted economy, and gray line corresponds to bank restricted economy.

holdings and wealth share drift between the rich and poor households. This is because of the endogenous increase in capital return spread, pushing up the first component of equation 5.1. In turn, higher return spread intensifies inequality dynamics: in response to a shock, the Gini coefficient raises more in regulated economies due to a combination of high risk exposure among the wealthy and high expected capital returns. The effect is especially more pronounced in the fund economy, where the capital return spread is the largest.

5.3 Revisiting Tradeoffs

Many researchers have emphasized a macro-prudential trade-off between growth and stabililty. We can see that our model also suggests such a tradeoff in Table 4. Tightening both the fund and bank leverage restrictions leads lower investment but also to lower consumption risk.

However, our analysis suggests that inequality is also an additional dimension in the macro-prudential tradeoff. Tightening the fund and bank leverage restrictions leads to higher inequality, as measured by the Gini coefficient for the economy. The intuition for this result can be seen in the change in the Sharpe Ratio and the fund contract spread (or annuity spread). Restricting the financial intermediaries ultimately opens up the risk premium and decreases the financing advantage of the fund sector. This is especially true when the fund is restricted because it is better suited to act as a backstop for the economy.

6 Counterfactual: Demographic change

Pension and insurance funds are inherently exposed to demographic risks because they are short mortality risk through the sale of annuities. Capital regulation further distorts their ability to absorb these risks: when longevity increases, annuity liabilities rise, but insurers often retrench rather than expand supply since regulatory capital charges make equity financing costly (Koijen and Yogo, 2016). On the demand side, demographic pressures also shape pension fund behavior. Rising longevity expands liabilities and underfunding, creating strong incentives to seek higher returns by tilting toward risky assets (Novy-Marx and Rauh, 2011). In this way, demographic-driven liability growth directly influences balance sheets and portfolio choices. To capture this mechanism, we study a mirror counterfactual economy with shorter household life spans that reduces longevity-driven liability pressure, modeled as an increase in the parameter λ_h. This allows us to quantify how demographic risks affect asset prices and household wealth distribution.

Figure 4 illustrates how demographic shifts sectoral balance sheets, portfolio allocations,

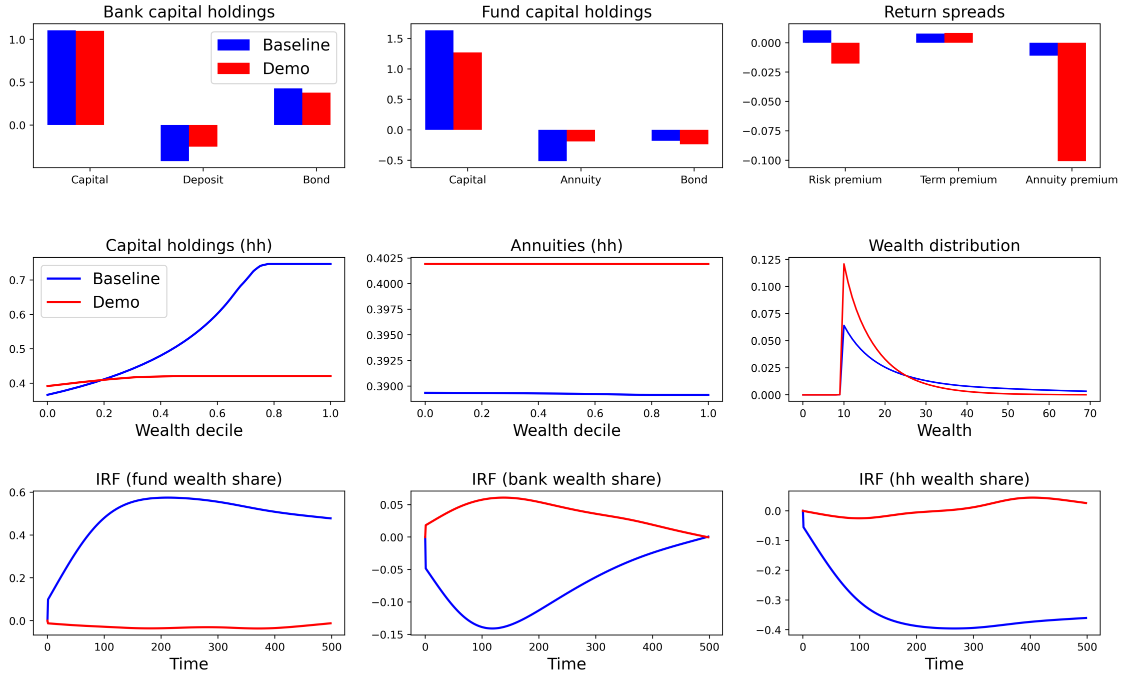

Figure 4: Demographic change: The top panel presents the financial sector portfolio holdings and return spreads. The second row presents household portfolio holdings and wealth distribution. The last row presents impulse response of sectoral wealth shares to a 2 s.d. negative TFP shock. In all plots, the blue represents baseline economy, and red represents a counterfactual economy with $\lambda_h = 0.15$.

Table 5: Counterfactual-2: Equilibrium Comparison Across Baseline economy with $\lambda = 0.10$, and a counterfactual economy with $\lambda_h = 0.15$

	Baseline	**Counterfactual**
Fund A/E	1.454	0.988
Bank A/E	1.536	1.284
Sharpe Ratio	1.649	-36.166
Term Premium (%)	0.785	-1.779
Conv. Yield (%)	0.275	-20.248
Govt. bond price	0.220	0.261
Annuity spread (%)	-1.106	-53.429
Output (%)	2.633	3.430
Investment (%)	11.785	26.352
Households		
Total consumption	0.703	0.591
Wealth	1.637	1.392
Gini Coefficient	0.156	0.073
Wealth (Top 1%/Median)	1.448	1.007
Cons. Risk (%)	4.197	4.221
Cons. Risk (Top 1%/Median)	1.034	1.167

and the distribution of household wealth, while Table 5 summarizes the corresponding moments. The counterfactual economy with a higher death rate produces notable changes in who acts as shock absorbers in downturns, alongside distributional changes across households. The most immediate effect of a higher death rate is the loss of household wealth share to the other agents in the economy. Because of high death risk, the demand for annuity and capital goes up, increasing their prices. In equilibrium, this translates to negative spreads. From the fund perspective, high prices reduce the attractiveness of capital. Therefore, they shrink their balance sheet by scaling down on capital, and retreating from their role as marginal risk absorbers. The vacuum left by the fund sector is taken by the banking sector. They expand their balance sheet by taking on more leverage, and in doing so, assume the stabilizing role during downturns that the funds played in the baseline economy. The larger banking sector improves their aggregate capacity to absorb shocks, which stabilizes capital prices more directly. The result is higher output and capital investment relative to the baseline economy.

The retreat of funds, however, has important consequences for the households. The shrinking of the fund sector means that households have limited access to annuities exactly when their need for it is most acute. On the other hand, the contraction of the fund sector and the shift in intermediation towards the banking sector produce a more even distribution of capital holdings across the households. Compared to the baseline economy, inequality is reduced, with a sharp reduction in the Gini coefficient and narrowing wealth between the top 1% and the median household. In this sense, the counterfactual economy delivers a more compressed distribution. However, this comes at the cost of lower consumption and wealth as a result of high annuity and capital prices. The risk exposure marginally increases due to high annuity return volatility. In sum, demographic shift trades off lower wealth inequality with lower consumption and wealth of the median household.

Taken together, our counterfactual results demonstrate that financial sector segmentation is not only an asset pricing phenomenon but also a central determinant of household welfare and inequality. Who absorbs risk in downturns, whether banks, funds, or households, critically shapes the trade-offs between growth, stability, and inequality. By embedding intermediary frictions into a heterogeneous agent framework, we show how regulation and demographics alter these channels in ways that standard representative agent or pricing-only models cannot capture.

More broadly, the paper contributes methodologically by showing that deep learning tools can overcome the curse of dimensionality in models that feature rich heterogeneity and complex dynamics. This opens the door for future work to study a wider class of policy questions where aggregate risk, institutional frictions, and inequality interact. In particular, extensions that allow intermediaries to raise outside equity, incorporate housing markets, or explore international spillovers could provide valuable insights into ongoing debates about the resilience of the financial system and the distributional consequences of macro financial policies.

7 Conclusion

This paper has examined how segmentation within the financial sector interacts with household heterogeneity to shape asset prices, stability, and inequality. We developed a new deep learning methodology that enables global solutions in environments with long-term assets, stochastic volatility, and binding portfolio constraints. This approach bridges advances in intermediary asset pricing and heterogeneous agent macroeconomics, providing a flexible framework for studying how regulation and demographics influence the joint distribution of wealth and asset market dynamics. Quantitatively, we calibrated the model to the post financial crisis United States economy from 2010 to 2024 and showed that it matches key macroeconomic, asset pricing, and cross sectional portfolio moments. The model reproduces realistic heterogeneity in capital holdings across households, delivers endogenous volatility in asset returns, and generates a fat tailed wealth distribution consistent with survey and administrative data. The interaction between intermediaries is central. Banks issue short term liabilities that remain stable in downturns, while funds issue long term annuities whose value falls in recessions, enabling them to expand balance sheets and absorb risk. This mechanism explains why funds act as stabilizers in the baseline economy but also why their behavior imposes costs on households through higher annuity premia.

Counterfactual experiments highlight the tradeoffs associated with alternative regulatory and demographic regimes. Fund regulation, which imposes bank style leverage limits, reduces volatility but raises inequality by shifting risk to households with greater capital exposure. Bank regulation, in the form of tighter capital requirements, instead amplifies volatility while also increasing inequality, as wider return spreads disproportionately benefit wealthier households. Demographic change operates through a different channel. Higher household mortality shifts risk absorption away from funds and toward banks. This compression of inequality comes at the expense of lower aggregate wealth and consumption, underscoring the complex role that demographics play in shaping both macroeconomic outcomes and distributional patterns.

References

Acharya, Viral V., Robert F. Engle, and Diane Pierret, "Testing Macroprudential Stress Tests: The Risk of Regulatory Risk Weights," *Journal of Monetary Economics*, 2014, *65*, 36–53.

Admati, Anat R. and Martin F. Hellwig, *The Bankers' New Clothes: What's Wrong with Banking and What to Do about It*, Princeton, NJ: Princeton University Press, 2013.

Azinovic, Marlon and Jan Žemlička, "Economics-Inspired Neural Networks with Stabilizing Homotopies," *arXiv preprint arXiv:2303.14802*, 2023.

_ , Luca Gaegauf, and Simon Scheidegger, "Deep equilibrium nets," *International Economic Review*, 2022, *63* (4), 1471–1525.

Bach, Laurent, Laurent E. Calvet, and Paolo Sodini, "Rich Pickings? Risk, Return, and Skill in Household Wealth," *American Economic Review*, September 2020, *110* (9), 2703–2747.

Basak, Suleyman and Domenico Cuoco, "An equilibrium model with restricted stock market participation," *The Review of Financial Studies*, 1998, *11* (2), 309–341.

— **and Georgy Chabakauri**, "Asset Prices, Wealth Inequality, and Taxation," *SSRN Electronic Journal*, 1 2024.

Begenau, Juliane, Pauline Liang, and Emil Siriwardane, "The Rise of Alternatives," Technical Report Working Paper 25-016, Harvard Business School August 2024.

Black, Lamont K., Ioannis Floros, and Rajdeep Sengupta, "Raising capital when the going gets tough: U.S. bank equity issuance from 2001 to 2014," *Research Working Paper*, 6 2016.

Blanchard, Olivier J, "Debt, deficits, and finite horizons," *Journal of political economy*, 1985, *93* (2), 223–247.

Bretscher, Lorenzo, Jesús Fernández-Villaverde, and Simon Scheidegger, "Ricardian Business Cycles," *Available at SSRN*, 2022.

Bricker, Jesse, Alice Henriques Volz, and Peter Hansen, "How Much Has Wealth Concentration Grown in the United States? A Re-Examination of Data from 2001-2013," Finance and Economics Discussion Series (FEDS) Working Paper 2018-024, Board of Governors of the Federal Reserve System June 2018.

Brunnermeier, Markus K and Yuliy Sannikov, "A macroeconomic model with a financial sector," *American Economic Review*, 2014, *104* (2), 379–421.

— **and** — , "Macro, money, and finance: A continuous-time approach," in "Handbook of Macroeconomics," Vol. 2, Elsevier, 2016, pp. 1497–1545.

Catherine, Sylvain, Max Miller, James Paron, and Natasha Sarin, "Who hedges interest-rate risk? Implications for wealth inequality," *SSRN Electronic Journal*, 01 2022.

Chan, Yeung Lewis and Leonid Kogan, "Catching up with the Joneses: Heterogeneous preferences and the dynamics of asset prices," *Journal of Political Economy*, 2002, *110* (6), 1255–1285.

Cioffi, Riccardo A, "Heterogeneous risk exposure and the dynamics of wealth inequality," *Working Paper*, 2021.

Coimbra, Nuno and Hélène Rey, "Financial Cycles with Heterogeneous Intermediaries," *The Review of Economic Studies*, mar 2024, *91* (2), 817–857.

Duarte, Victor, Diogo Duarte, and Dejanir H Silva, "Machine Learning for Continuous-Time Finance," *The Review of Financial Studies*, 09 2024, *37* (11), 3217–3271.

Fagereng, Andreas, Luigi Guiso, Davide Malacrino, and Luigi Pistaferri, "Heterogeneity and Persistence in Returns to Wealth," *Econometrica*, 2020, *88* (1), 115–170.

_ **, Matthieu Gomez, Emilien Gouin-Bonenfant, Martin Holm, Benjamin Moll, and Gisle Natvik**, "Asset-price redistribution," Technical Report, Working Paper 2022.

Favilukis, Jack, "Inequality, stock market participation, and the equity premium," *Journal of Financial Economics*, 2013, *107* (3), 740–759.

Fernández-Villaverde, Jesús and Oren Levintal, "The Distributional Effects of Asset Returns," *Working Paper.*, 2024.

_ **, Samuel Hurtado, and Galo Nuno**, "Financial frictions and the wealth distribution," *Econometrica*, 2023, *91* (3), 869–901.

Fernández-Villaverde, Jesús, Joël Marbet, Galo Nuño, and Omar Rachedi, "Inequality and the Zero Lower Bound," CESifo Working Paper Series 10471, CESifo 5 2023.

_ **, Samuel Hurtado, and Galo Nuño**, "Financial Frictions and the Wealth Distribution," *Econometrica*, 2023, *91* (3), 869–901.

Gaudio, Francesco Saverio, "Stock Market Participation and Macro-Financial Trends," Technical Report —, WBS Finance Group Research Paper October 2024.

_ **, Ivan Petrella, and Emiliano Santoro**, "Asset Market Participation, Redistribution, and Asset Pricing," Discussion Paper / SSRN Working Paper DP No. 17984, Centre for Economic Policy Research (CEPR) – WBS Finance Group December 2023.

Gertler, Mark, Nobuhiro Kiyotaki, and Andrea Prestipino, "A Macroeconomic Model with Financial Panics," *The Review of Economic Studies*, 05 2019, *87* (1), 240–288.

Gomes, Francisco J. and Alexander Michaelides, "Asset Pricing with Limited Risk Sharing and Heterogeneous Agents," *Review of Financial Studies*, 2007, *21* (1), 415–448.

Gomez, Matthieu, "Asset Prices and Wealth Inequality," 2017 Meeting Papers 1155, Society for Economic Dynamics 2017.

_ **and Émilien Gouin-Bonenfant**, "Wealth inequality in a low rate environment," *Econometrica*, 2024, *92* (1), 201–246.

Gopalakrishna, Goutham, "Aliens and continuous time economies," *Swiss Finance Institute Research Paper*, 2021, *21* (34).

Greenwood, Robin and Annette Vissing-Jorgensen, "The Impact of Pensions and Insurance on Global Yield Curves," Finance Working Paper 19-059, Harvard Business School 2018. HBS Finance Working Paper No. 19-059.

Gu, Zhouzhou, Methieu Laurière, Sebastian Merkel, and Jonathan Payne, "Deep Learning Solutions to Master Equations for Continuous Time Heterogeneous Agent Macroeconomic Models," *Princeton Working Paper*, 2023.

Guvenen, Fatih, "A parsimonious macroeconomic model for asset pricing," *Econometrica*, 2009, *77* (6), 1711–1750.

Han, Jiequn, Arnulf Jentzen, and Weinan E, "Solving high-dimensional partial differential equations using deep learning," *Proceedings of the National Academy of Sciences*, 2018, *115* (34), 8505–8510.

_ , Yucheng Yang, and Weinan E, "Deepham: A global solution method for heterogeneous agent models with aggregate shocks," *arXiv preprint arXiv:2112.14377*, 2021.

He, Zhiguo and Arvind Krishnamurthy, "Intermediary asset pricing," *American Economic Review*, 2013, *103* (2), 732–770.

Huang, Ji, "A Probabilistic Solution to High-Dimensional Continuous-Time Macro-Finance Models," *Available at SSRN 4122454*, 2022.

_ , "Breaking the Curse of Dimensionality in Heterogeneous-Agent Models: A Deep Learning-Based Probabilistic Approach," *SSRN Working Paper*, 2023.

Internal Revenue Service, Statistics of Income Division, "Estate Tax Statistics," Technical Report, U.S. Department of the Treasury 2023.

Irie, Magnus, "Innovations in Entrepreneurial Finance," *SSRN Working Paper.*, 2024.

Kahou, Mahdi Ebrahimi, Jesús Fernández-Villaverde, Jesse Perla, and Arnav Sood, "Exploiting symmetry in high-dimensional dynamic programming," Technical Report, National Bureau of Economic Research 2021.

Kargar, Mahyar, "Heterogeneous intermediary asset pricing," *Journal of Financial Economics*, 8 2021, *141*, 505–532.

Khorrami, Paymon, "Entry and Slow-Moving Capital: Using Asset Markets to Infer the Costs of Risk Concentration," Technical Report, SSRN Working Paper 2021. Available at SSRN 2777747.

Koijen, Ralph S. J. and Motohiro Yogo, "The Impact of Financial Regulation on Insurance Markets," *American Economic Review*, 2016, *106* (1), 347–376.

Koijen, Ralph S. J and Motohiro Yogo, "The Evolution from Life Insurance to Financial Engineering," Working Paper 29030, National Bureau of Economic Research July 2021.

Koijen, Ralph S. J. and Motohiro Yogo, "Understanding the Ownership Structure of Corporate Bonds," *American Economic Review: Insights*, 3 2023, *5*, 73–92.

Koijen, Ralph SJ and Motohiro Yogo, "A demand system approach to asset pricing," *Journal of Political Economy*, 2019, *127* (4), 1475–1515.

Koijen, Ralph S.J. and Motohiro Yogo, "The Fragility of Market Risk Insurance," *The Journal of Finance*, 4 2022, *77*, 815–862.

Krishnamurthy, Arvind and Wenhao Li, "Dissecting Mechanisms of Financial Crises: Intermediation and Sentiment," Working Paper 27088, National Bureau of Economic Research May 2020.

Krusell, Per and Anthony A Smith, "Income and Wealth Heterogeneity in the Macroeconomy," *Journal of Political Economy*, 1998, *106* (5), 867–896.

Kubler, Felix and Simon Scheidegger, "Self-justi ed equilibria: Existence and computation," 2018 Meeting Papers 694, Society for Economic Dynamics 11 2018.

Lansing, Kevin J., "Asset Pricing with Concentrated Ownership of Capital and Distribution Shocks," *American Economic Journal: Macroeconomics*, October 2015, *7* (4), 67–103.

Maliar, Lilia, Serguei Maliar, and Pablo Winant, "Deep learning for solving dynamic economic models.," *Journal of Monetary Economics*, 2021, *122*, 76–101.

Maxted, Peter, "A Macro-Finance Model with Sentiment," *The Review of Economic Studies*, 03 2023.

Mitchell, Olivia S., James M. Poterba, Mark J. Warshawsky, and Jeffrey R. Brown, "New Evidence on the Money's Worth of Individual Annuities," *Brookings Papers on Economic Activity*, 1999, *1999* (2), 131–192.

Novy-Marx, Robert and Joshua D. Rauh, "Public Pension Promises: How Big Are They and What Are They Worth?," *Journal of Finance*, 2011, *66* (4), 1211–1249.

Office, Congressional Budget, "Options for Changing the Tax Treatment of Charitable

Giving," Technical Report, Congressional Budget Office May 2017.

Saez, Emmanuel and Gabriel Zucman, " Wealth Inequality in the United States since 1913: Evidence from Capitalized Income Tax Data," *The Quarterly Journal of Economics*, 02 2016, *131* (2), 519–578.

Sauzet, Maxime, "Projection methods via neural networks for continuous-time models," *Available at SSRN 3981838*, 2021.

Vayanos, Dimitri and Jean-Luc Vila, "A Preferred-Habitat Model of the Term Structure of Interest Rates," *Econometrica*, 1 2021, *89*, 77–112.

Òscar Jordà, "Estimation and Inference of Impulse Responses by Local Projections," *American Economic Review*, March 2005, *95* (1), 161–182.

A Recursive Characterization of Equilibrium

The finite dimensional aggregate state variables are: $\boldsymbol{s} := (z, K, \eta_b, \eta_f)$, where η_j is the fraction of wealth held by sector $j \in \{b, f\}$. We also have that the infinite dimensional state variable: g_h. With some abuse of notation, we let $G = \{\eta_b, \eta_f, g_h\}$ denote the collection of distribution state variables in the economy. The belief about prices becomes the belief about the evolution of sector wealth, $(\tilde{\mu}_{\eta,j}, \tilde{\sigma}_{\eta,j})_{j\in\{h,f\}}$, and the evolution of the household measure function g_h. For convenience, we define the following notation (all summarized here):

$$
\begin{aligned}
\boldsymbol{s} &:= (z, K, \eta_b, \eta_f) \\
\boldsymbol{S} &:= (\boldsymbol{s}, g_h) \\
\boldsymbol{x} &:= (a, z, K, \eta_b, \eta_f) \\
\boldsymbol{X} &:= (\boldsymbol{x}, g_h)
\end{aligned}
$$

Let $V_i(\boldsymbol{X})$ denote the value function for agent of type $i \in \{h, b, f\}$ with state variable $\boldsymbol{X}$.

In matrix form, the evolution of $\boldsymbol{x}_t$ is (under household beliefs):

$$
d\boldsymbol{x}_t = (\boldsymbol{\mu}_x(\boldsymbol{x}_t, c_h, \boldsymbol{\theta}_h) \odot \boldsymbol{x}_t)dt + (\boldsymbol{\sigma}_x(\boldsymbol{x}_t, \boldsymbol{\theta}_h) \odot \boldsymbol{x}_t)^T dW_t
$$

where

$$
\boldsymbol{\mu}_x(\boldsymbol{x}, c_h, \boldsymbol{\theta}_h) = \begin{bmatrix} \mu_a(x, c_h, \boldsymbol{\theta}_h) \\ \mu_z \\ \mu_K \\ \tilde{\mu}_{\eta_b} \\ \tilde{\mu}_{\eta_f} \end{bmatrix}, \qquad \boldsymbol{\sigma}_x(\boldsymbol{x}, \boldsymbol{\theta}_h)^T = \begin{bmatrix} \sigma_{a,z}(\boldsymbol{x}, \boldsymbol{\theta}_h) \\ \sigma_z \\ 0 \\ \tilde{\sigma}_{\eta_b,z} \\ \tilde{\sigma}_{\eta_f,z} \end{bmatrix}
$$

where $\sigma_{y,z}$ is the vector of volatilities for variable y project to z shock. And (dropping explicit dependence on $\boldsymbol{x}$ to save space) we have:

$$
\begin{aligned}
\Sigma &= \boldsymbol{\sigma}_x \boldsymbol{\sigma}_x^T(\boldsymbol{x}, \boldsymbol{\theta}_h) \\
&= \begin{bmatrix} \sigma_a^2(\boldsymbol{\theta}_h) & \sigma_a(\boldsymbol{\theta}_h)\sigma_z & 0 & \sigma_a(\boldsymbol{\theta}_h)\tilde{\sigma}_{\eta_h} & \sigma_a(\boldsymbol{\theta}_h)\tilde{\sigma}_{\eta_f} \\ \sigma_z\sigma_{a,z}(\boldsymbol{\theta}_h) & \sigma_z^2 & 0 & \sigma_z\tilde{\sigma}_{\eta_b,z} & \sigma_z\tilde{\sigma}_{\eta_f,z} \\ 0 & 0 & 0 & 0 & 0 \\ \tilde{\sigma}_{\eta_b}\sigma_a & \tilde{\sigma}_{\eta_b,z}\sigma_z & 0 & \tilde{\sigma}_{\eta_b}^2 & \tilde{\sigma}_{\eta_b}\tilde{\sigma}_{\eta_f} \\ \tilde{\sigma}_{\eta_f}\sigma_a & \tilde{\sigma}_{\eta_f,z}\sigma_z & 0 & \tilde{\sigma}_{\eta_f}\tilde{\sigma}_{\eta_b} & \tilde{\sigma}_{\eta_f}^2 \end{bmatrix}
\end{aligned}
$$

We use analogous notation for the law of motion for $\boldsymbol{s}_t$. Agent's belief about the law of motion of $g_{h,t}$ is denoted by:

$$dg_{h,t}(a) = \tilde{\mu}_g(a, \boldsymbol{S})dt + \tilde{\sigma}_g(a, \boldsymbol{S})^T dW_t$$

A.1 Household Optimization

HBJE: Given beliefs about the evolution of the wealth shares, the household value function $V_h(a, \cdot)$ solves the HJBE (A.1) below (written in matrix form):

$$\begin{aligned}
\rho_h V_h(\boldsymbol{X}) = \max_{c_h, \boldsymbol{\theta}_h, \iota_h} \Big\{ & u(c_h) + (\psi_{h,k}(\theta_h^k) + \psi_{h,n}(\theta_h^n))\Xi_h a \\
& + \lambda \left(\mathcal{U}\left(a\mathcal{W}(\theta_{h,t}^k, \theta_h^n) \right) - V_h(\boldsymbol{X}) \right) \\
& + (\boldsymbol{\mu}_x(\boldsymbol{x}, c_h, \boldsymbol{\theta}_h, \iota_h) \odot \boldsymbol{x})^T D_x V_h(\boldsymbol{X}) \\
& + \frac{1}{2}\mathrm{tr}\left\{ (\boldsymbol{\sigma}_x(\boldsymbol{x}, \boldsymbol{\theta}_h) \odot \boldsymbol{x})^T (\boldsymbol{\sigma}_x(\boldsymbol{x}, \boldsymbol{\theta}_h) \odot \boldsymbol{x}) D_x^2 V_h(\boldsymbol{X}) \right\} \\
& + \mathcal{L}_g V_h(\boldsymbol{X}) \Big\},
\end{aligned} \tag{A.1}$$

where $\mathcal{L}_g V_h(\boldsymbol{X})$ is the collection of Frechet derivative terms and:

$$D_x V_h(\boldsymbol{x}) = \begin{bmatrix} \partial_a V_h(\boldsymbol{x}) \\ \partial_z V_h(\boldsymbol{x}) \\ \partial_K V_h(\boldsymbol{x}) \\ \partial_{A_h} V_h(\boldsymbol{x}) \\ \partial_{A_b} V_h(\boldsymbol{x}) \\ \partial_{A_f} V_h(\boldsymbol{x}) \end{bmatrix}, \qquad D_x^2 V_h(\boldsymbol{x}) = \begin{bmatrix} \partial^2_{aa} V_h & \dots & \partial^2_{aA_f} V_h \\ \partial^2_{za} V_h & \dots & \partial^2_{zA_f} V_h \\ \partial^2_{Ka} V_h & \dots & \partial^2_{KA_f} V_h \\ \partial^2_{A_h a} V_h & \dots & \partial^2_{A_h A_f} V_h \\ \partial^2_{A_b a} V_h & \dots & \partial^2_{A_b A_f} V_h \\ \partial^2_{A_f a} V_h & \dots & \partial^2_{A_f A_f} V_h \end{bmatrix}$$

and $\mathcal{W}(\theta_h^k, \theta_h^n)$ corresponds to the optimal terminal consumption bundle when the retirement shock hits $\mathcal{W}(\theta_{h,t}^k, \theta_h^n) = ((q^n)^{-1}\theta_h^n)$.

HBJE (partial matrix): We can rewrite the HJBE with the controlled variables taken out of the matrices. Then the HJBE is given by:

$$
\begin{aligned}
\rho_h V_h(a,\boldsymbol{s},g_h) = \max_{c_h,\boldsymbol{\theta}_h,\iota_h} \Big\{ & u(c_h) + (\psi_{h,k}(\theta_h^k) + \psi_{h,d}(\theta_h^d))\Xi_h a \\
& + \lambda\left(\mathcal{U}\left(a\mathcal{W}(\theta_{h,t}^k,\theta_h^n)\right) - V_h(a,\boldsymbol{s},g_h)\right) \\
& + \mu_a(a,\boldsymbol{s},c_h,\boldsymbol{\theta}_h,\iota_h)a + (\boldsymbol{\mu}_s(\boldsymbol{s},g_h)\odot\boldsymbol{s})^T D_s V_h(a,\boldsymbol{s},g_h) \\
& + \frac{1}{2}\partial_{aa}^2 V_h(a,\boldsymbol{s},g_h)\sigma_a^2(\boldsymbol{\theta}_h,\boldsymbol{s},g_h)a^2 + \sum_j \partial_{as_j} V_h(a,\boldsymbol{s},g_h)\sigma_a(\boldsymbol{\theta}_h,\boldsymbol{s},g_h)\sigma_{s_j} a s_j \\
& + \frac{1}{2}\mathrm{tr}\left\{(\boldsymbol{\sigma}_s(\boldsymbol{s},g_h)\odot\boldsymbol{s})^T(\boldsymbol{\sigma}_s(\boldsymbol{s},g_h)\odot\boldsymbol{s})D_s^2 V_h(a,\boldsymbol{s},g_h)\right\} + \mathcal{L}_g V_h(a,\boldsymbol{s},g_h)\Big\}
\end{aligned}
$$

where:

$$
\begin{aligned}
\psi_h(\theta_{h,t}^k) &= \frac{\bar{\psi}_k}{2}\left(\theta_{h,t}^k\right)^2 \\
\psi_h(\theta_{h,t}^d) &= \frac{\bar{\psi}_d}{2}\left(\theta_{h,t}^d\right)^2 \\
\mu_a(a,c_h,\boldsymbol{\theta}_h,\cdot) &= \left(\tilde{r}_t^d + \theta_{h,t}^n(\tilde{r}_t^n - \tilde{r}_t^d) + \theta_{h,t}^k(\tilde{r}_t^k - \tilde{r}_t^d) - c_{h,t}/a_{h,t} - \tau_{h,t}\right) \\
\sigma_a(\boldsymbol{\theta}_h,\cdot) &= \boldsymbol{\theta}_h^T\tilde{\sigma}_q = \theta_h^n\tilde{\sigma}_{q^n,z} + \theta_h^k\tilde{\sigma}_{q^k,z}
\end{aligned}
$$

and so:

$$
\begin{aligned}
\sigma_a^2(a,\boldsymbol{\theta}_h,\cdot) &= (\theta_h^n\tilde{\sigma}_{q^n,z} + \theta_{h,t}^k\tilde{\sigma}_{q^k,z})^2 \\
\sigma_a(a,\boldsymbol{\theta}_h,\cdot)\tilde{\sigma}_{\eta_j} &= (\theta_{h,t}^n\tilde{\sigma}_{q^n,z} + \theta_h^k\tilde{\sigma}_{q^k,z})\tilde{\sigma}_{\eta_j,z} \\
\sum_j \partial_{as_j} V_h(a,\boldsymbol{s})\boldsymbol{\sigma}_a^T(\boldsymbol{\theta}_h,\boldsymbol{s})\boldsymbol{\sigma}_{s_j} &= \partial_{az}^2 V_h(a,\boldsymbol{s})\sigma_{a,z}(\boldsymbol{\theta}_h,\boldsymbol{s})\sigma_z a z + \sum_j \partial_{aA_j}^2 V_h(a,\boldsymbol{s})\boldsymbol{\sigma}_a^T(\boldsymbol{\theta}_h,\boldsymbol{s})\tilde{\boldsymbol{\sigma}}_{A_j}(\boldsymbol{s})a\eta_j
\end{aligned}
$$

The HJBE becomes:

$$
\begin{aligned}
\rho_h V_h(a,\boldsymbol{s}) = \max_{c_h,\boldsymbol{\theta}_h,\iota_h} \Big\{ & u(c_h) + (\psi_{h,k}(\theta_h^k) + \psi_{h,n}(\theta_h^n))\Xi_h a \\
& + \lambda\left(\mathcal{U}\left(a\mathcal{W}\left(\theta_h^k,\theta_h^n\right)\right) - V_h(a,\boldsymbol{s})\right) \\
& + \mu_a(a,\boldsymbol{s},c_h,\boldsymbol{\theta}_h,\iota_h)a + (\boldsymbol{\mu}_s(\boldsymbol{s})\odot\boldsymbol{s})^T D_s V_h(a,\boldsymbol{s}) \\
& + \frac{1}{2}\partial_{aa}^2 V_h(a,\boldsymbol{s})(\boldsymbol{\theta}_h^T\tilde{\boldsymbol{\sigma}}_q)^2 a^2 + \sum_j \partial_{as_j} V_h(a,\boldsymbol{s})\boldsymbol{\theta}_h^T\tilde{\boldsymbol{\sigma}}_q\sigma_{s_j} a s_j \\
& + \frac{1}{2}\mathrm{tr}\left\{(\boldsymbol{\sigma}_s(\boldsymbol{s})\odot\boldsymbol{s})^T(\boldsymbol{\sigma}_s(\boldsymbol{s})\odot\boldsymbol{s})D_s^2 V_h(a,\boldsymbol{s})\right\} + \mathcal{L}_g V_h(a,\boldsymbol{s},g_h) + \mathcal{L}_g V_h(a,\boldsymbol{s},g_h)\Big\}
\end{aligned}
$$

FOCs: The first order conditions are given by (as as the problem with out the household distribution):

$$
\begin{aligned}
[c_h]: \qquad & 0 = u'(c_h) - \partial_a V_h \\
[\iota_h]: \qquad & 0 = \Phi'(\iota) - \frac{1}{q_t^k} \\
[\theta_h^k]: \qquad & 0 = \partial_a V_h(\tilde{r}^k - \tilde{r}^d)a + \lambda \partial_{\theta_h^k} \mathcal{W}(\theta_h^k, \theta_h^n)\mathcal{U}'(\mathcal{C}) \\
& \quad + \partial_{\theta_h^k} \psi_{h,k} \Xi_h a + \partial_{aa} V_h \tilde{\sigma}_{q^k} \sigma_a a^2 + \sum_j \partial_{as_j} V_h \tilde{\sigma}_{q^k} \sigma_{s_j} a s_j \\
& = \partial_a V_h(\tilde{r}^k - \tilde{r}^d)a + \lambda \partial_{\theta_h^k} \mathcal{W}(\theta_h^k, \theta_h^n)\mathcal{U}'(\mathcal{C}) \\
& \quad + \partial_{\theta_h^k} \psi_{h,k} \Xi_h a + (D_x(\partial_a V_h)^T (\boldsymbol{\sigma}_x \odot \boldsymbol{x}))^T \tilde{\sigma}_{q^k} a \\
[\theta_h^n]: \qquad & 0 = \partial_a V_h(\tilde{r}^n - \tilde{r}^d)a + \lambda \partial_{\theta_h^n} \mathcal{W}(\theta_h^k, \theta_h^n)\mathcal{U}'(\mathcal{C}) \\
& \quad + \partial_{\theta_h^n} \psi_{h,n} \Xi_h a + \partial_{aa} V_h \tilde{\sigma}_{q^n} \sigma_a a^2 + \sum_j \partial_{as_j} V_h \tilde{\sigma}_{q^n} \sigma_{s_j} a s_j \\
& = \partial_a V_h(\tilde{r}^n - \tilde{r}^d)a + \lambda \partial_{\theta_h^n} \mathcal{W}(\theta_h^k, \theta_h^n)\mathcal{U}'(\mathcal{C}) \\
& \quad + \partial_{\theta_h^n} \psi_{h,k} \Xi_h a + (D_x(\partial_a V_h)^T (\boldsymbol{\sigma}_x \odot \boldsymbol{x}))^T \tilde{\sigma}_{q^n} a
\end{aligned}
$$

SDF Evolution: Let $\xi_h(\boldsymbol{X}) := \partial_a V_h(a, \boldsymbol{s}, g_h)$. From Ito's Lemma, we have that the drift and volatility of ξ_h are given by:

$$
\begin{aligned}
\mu_{\xi_h} \xi_h(\boldsymbol{X}) &= (D_x \xi_h(\boldsymbol{X}))^T \boldsymbol{\mu}_x \\
& \quad + \frac{1}{2} \mathrm{tr} \left\{ (\boldsymbol{\sigma}_x(\boldsymbol{X}, \boldsymbol{\theta}_h) \odot \boldsymbol{X})^T (\boldsymbol{\sigma}_x(\boldsymbol{X}, \boldsymbol{\theta}_h) \odot \boldsymbol{x}) D_x^2 \xi_h(\boldsymbol{X}) \right\} \\
& \quad + \mathcal{L}_g \xi_h(\boldsymbol{X}) \\
&= \partial_a \xi_h(a, \boldsymbol{s}, g_h) \mu_a(a, c_h, \boldsymbol{\theta}_h, \boldsymbol{s}, g_h) a \\
& \quad + (D_s \xi_h(a, \boldsymbol{s}, g_h))^T (\boldsymbol{\mu}_s(\boldsymbol{s}) \odot \boldsymbol{s}) \\
& \quad + \frac{1}{2} \partial_{aa}^2 \xi_h(a, \boldsymbol{s}, g_h) \sigma_a^2(\boldsymbol{\theta}_h, \boldsymbol{s}, g_h) a^2 \\
& \quad + \sum_j \partial_{as_j} \xi_h(a, \boldsymbol{s}, g_h) \sigma_a(\boldsymbol{\theta}_h, \boldsymbol{s}, g_h) \sigma_{s_j} a s_j \\
& \quad + \frac{1}{2} \mathrm{tr} \left\{ (\boldsymbol{\sigma}_s(\boldsymbol{s}) \odot \boldsymbol{s})^T (\boldsymbol{\sigma}_s(\boldsymbol{s}) \odot \boldsymbol{s}) D_s^2 \xi_h(a, \boldsymbol{s}, g_h) \right\} + \mathcal{L}_g \xi_h(\boldsymbol{X}) \\
\sigma_{\xi_h} \xi_h &= (\boldsymbol{\sigma}_x \odot \boldsymbol{x})^T (D_x \xi_h) \\
&= \ \partial_a \xi_h \sigma_{a,z} a + \partial_z \xi_h \sigma_z z + \textstyle\sum_j \partial_{a_j} \xi_h \sigma_{a_j,z} \eta_j
\end{aligned}
$$

Thus, we can rewrite the FOCs as:

$$
\begin{aligned}
[\theta_h^k]: \qquad & 0 = \xi_h(\tilde{r}^n - \tilde{r}^d) + \lambda \partial_{\theta_h^k} \mathcal{W}(\theta_h^k, \theta_h^n) \frac{\mathcal{U}'(\mathcal{C})}{a} \\
& \quad + \partial_{\theta_h^k} \psi_{h,k} \Xi_h + (\sigma_{\xi_h} \xi_h)^T \sigma_{q^k} \\
[\theta_h^n]: \qquad & 0 = \xi_h(\tilde{r}^n - \tilde{r}^d) + \lambda \partial_{\theta_h^n} \mathcal{W}(\theta_h^k, \theta_h^n) \frac{\mathcal{U}'(\mathcal{C})}{a} + \partial_{\theta_h^n} \psi_{h,n} \Xi_h + (\sigma_{\xi_h} \xi_h)^T \sigma_{q^n}
\end{aligned}
$$

Imposing belief consistency and using the equilibrium result that $\Xi_h = \xi_h$, we get the simplified FOCs:

$$
\begin{aligned}
[\theta_h^k]: \qquad & r^k - r^d = -\lambda \partial_{\theta_h^k} \mathcal{W}(\theta_h^k, \theta_h^n) \frac{\mathcal{U}'(\mathcal{C})}{a\xi_h} - \partial_{\theta_h^k} \psi_{h,k} - \sigma_{\xi_h} \sigma_{q^k} \\
[\theta_h^n]: \qquad & r^n - r^d = -\lambda \partial_{\theta_h^n} \mathcal{W}(\theta_h^k, \theta_h^n) \frac{\mathcal{U}'(\mathcal{C})}{a\xi_h} - \partial_{\theta_h^n} \psi_{h,n} - \sigma_{\xi_h} \sigma_{q^n}
\end{aligned}
$$

Euler equation: We close this section by using the Envelope theorem to get the Euler equation (using the partial matrix representation). To do this, we treat θa as the choice rather than θ when taking the envelope theorem. This gives:

$$
\begin{aligned}
& \rho_h \xi_h(a, \boldsymbol{s}) \\
& \quad = (\psi_{h,k}(\theta_h^k a/a) + \psi_{h,n}(\theta_h^n a/a)) \Xi_h \\
& \qquad - \left(\partial_{\theta_h^k} \psi_{h,k}(\theta_h^k a/a) \frac{\theta_h^k}{a} + \partial_{\theta_h^k} \psi_{n,k}(\theta_h^n a/a) \frac{\theta_h^n}{a} \right) \Xi_h a \\
& \qquad - \lambda \xi_h(a, \boldsymbol{s}) + \partial_a \xi_h(a, \boldsymbol{s}) \mu_a(a, c_h, \boldsymbol{\theta}_h, \cdot) a + \xi_h(a, \boldsymbol{s})(r^d + \tau_h) \\
& \qquad + (D_s \xi_h(a, \boldsymbol{s}))^T (\boldsymbol{\mu}_s(\boldsymbol{s}) \odot \boldsymbol{s}) \\
& \qquad + \frac{1}{2} \partial_{aa}^2 \xi_h(a, \boldsymbol{s}) \sigma_a^2(\boldsymbol{\theta}_h, \boldsymbol{s}) a^2 \\
& \qquad + \sum_j \partial_{a s_j} \xi_h(a, \boldsymbol{s}) \sigma_a(\boldsymbol{\theta}_h, \boldsymbol{s}) \sigma_{s_j} a s_j \\
& \qquad + \frac{1}{2} \mathrm{tr} \left\{ (\boldsymbol{\sigma}_s(\boldsymbol{s}) \odot \boldsymbol{s})^T (\boldsymbol{\sigma}_s(\boldsymbol{s}) \odot \boldsymbol{s}) D_s^2 \xi_h(a, \boldsymbol{s}) \right\} + \mathcal{L}_g \xi_h \\
& \quad = (\psi_{h,k}(\theta_h^k) - \partial_{\theta_h^k} \psi_{h,k}(\theta_h^k a/a) \theta_h^k + \psi_{h,n}(\theta_h^n) - \partial_{\theta_h^k} \psi_{n,k}(\theta_h^n a/a) \theta_h^n) \Xi_h \\
& \qquad - \lambda \xi_h(a, \boldsymbol{s}) + (D_s \xi_h(\boldsymbol{x}))^T (\boldsymbol{\mu}_x(\boldsymbol{x}) \odot \boldsymbol{x}) + \xi_h(a, \boldsymbol{s}) \left(r^d + \tau_h \right) \\
& \qquad + \frac{1}{2} \mathrm{tr} \left\{ (\boldsymbol{\sigma}_x(\boldsymbol{x}, \boldsymbol{\theta}_h) \odot \boldsymbol{x})^T (\boldsymbol{\sigma}_x(\boldsymbol{x}, \boldsymbol{\theta}_h) \odot \boldsymbol{x}) D_x^2 \xi_h(\boldsymbol{x}) \right\} + \mathcal{L}_g \xi_h \\
& \quad = (\psi_{h,k}(\theta_h^k) - \partial_{\theta_h^k} \psi_{h,k}(\theta_h^k) \theta_h^k + \psi_{h,n}(\theta_h^n) - \partial_{\theta_h^n} \psi_{n,k}(\theta_h^n) \theta_h^n) \Xi_h \\
& \qquad - \lambda_h \xi_h(a, \boldsymbol{s}) + \mu_{\xi_h} \xi_h(a, \boldsymbol{s}) + \xi_h(a, \boldsymbol{s}) \left(r^d - \tau_h \right)
\end{aligned}
$$

So, imposing belief consistency and we get that:

$$\rho_h + \lambda_h = \mu_{\xi_h} + r^d - \tau_h + \psi_{h,k}(\theta_h^k) - \partial_{\theta_h^k}\psi_{h,k}(\theta_h^k)\theta_h^k + \psi_{h,n}(\theta_h^n) - \partial_{\theta_h^n}\psi_{n,k}(\theta_h^n)\theta_h^n$$

A.1.1 Banker Optimization

The banker HJBE is given by:

$$\begin{aligned}\rho_b V_b(a, \boldsymbol{s}, g_h) = \max_{c_b, \boldsymbol{\theta}_b, \iota_b} \Big\{ & u(c_b) + \mu_a(a, \boldsymbol{s}, c_b, \boldsymbol{\theta}_b, \iota_b)a + (\boldsymbol{\mu}_s(\boldsymbol{s}) \odot \boldsymbol{s})^T D_s V_b(a, \boldsymbol{s}, g_h) \\ & + \frac{1}{2}\partial_{aa}^2 V_b(a, \boldsymbol{s}, g_h)\sigma_a^2(\boldsymbol{\theta}_b, \boldsymbol{s})a^2 + \sum_j \partial_{as_j} V_b(a, \boldsymbol{s}, g_h)\sigma_a(\boldsymbol{\theta}_b, \boldsymbol{s})\sigma_{s_j} a s_j \\ & + \frac{1}{2}\mathrm{tr}\left\{(\boldsymbol{\sigma}_s(\boldsymbol{s}) \odot \boldsymbol{s})^T(\boldsymbol{\sigma}_s(\boldsymbol{s}) \odot \boldsymbol{s}) D_s^2 V_b(a, \boldsymbol{s})\right\} + \mathcal{L}_g V_b(a, \boldsymbol{s}, g_h) + \left[\psi_{b,k}(\theta_b^k) + \psi_{b,m}(\theta_b^m)\right]\xi_b a_b \Big\}\end{aligned}$$

where:

$$\begin{aligned}\mu_a(a, c_b, \theta_b, \cdot) &= \left(\tilde{r}^d + \theta_h^k(\tilde{r}^k - \tilde{r}^d) - c_{b,t}/a_b - \tau_b\right) \\ \sigma_a(\theta_b, \cdot) &= \theta_b^k \tilde{\sigma}_{q^k,z} + \theta_b^m \tilde{\sigma}_{q^m,z}\end{aligned}$$

Following the same steps, the equilibrium FOCs for the banker are given by:

$$\begin{aligned}[c_b]: &\qquad 0 = u'(c_b) - \partial_a V_b(a, \boldsymbol{s}, g_h) \\ [\iota_b]: &\qquad 0 = \Phi'(\iota) - \frac{1}{q_t^k} \\ [\theta_b^k]: &\qquad 0 = r^k - r^d + \sigma_{\xi_b}\sigma_{q^k,z} + \partial_{\theta_b^k}\psi_{b,k} \\ [\theta_b^m]: &\qquad 0 = r^m - r^d + \sigma_{\xi_b}\sigma_{q^m,z} + \partial_{\theta_b^m}\psi_{b,m}\end{aligned}$$

and the Euler equation is:

$$\rho_b = \mu_{\xi_b} + r^d - \tau_b + \left[\psi_{b,k} + \psi_{b,m} - \partial_{\theta_b^k}\psi_{b,k}\theta_b^k - \partial_{\theta_b^m}\psi_{b,m}\theta_b^m\right]$$

A.1.2 Fund Manager Optimization

The banker HJBE is given by:

$$\rho_f V_f(a, \boldsymbol{s}, g_h) = \max_{c_f, \boldsymbol{\theta}_f, \iota_f} \Big\{ u(c_f) + \mu_a(a, \boldsymbol{s}, c_f, \boldsymbol{\theta}_f, \iota_f) a + (\boldsymbol{\mu}_s(\boldsymbol{s}) \odot \boldsymbol{s})^T D_s V_f(a, \boldsymbol{s}, g_h)$$
$$+ \frac{1}{2}\partial^2_{aa} V_f(a, \boldsymbol{s}) \sigma_a^2(\boldsymbol{\theta}_f, \boldsymbol{s}, g_h) a^2 + \sum_j \partial_{a s_j} V_f(a, \boldsymbol{s}, g_h) \sigma_a(\boldsymbol{\theta}_f, \boldsymbol{s}) \sigma_{s_j} a s_j$$
$$+ \frac{1}{2}\mathrm{tr}\left\{ (\boldsymbol{\sigma}_s(\boldsymbol{s}) \odot \boldsymbol{s})^T (\boldsymbol{\sigma}_s(\boldsymbol{s}) \odot \boldsymbol{s}) D_s^2 V_f(a, \boldsymbol{s}, g_h) \right\} + \mathcal{L}_g V_f(a, \boldsymbol{s}, g_h) + \Big[\psi_{f,k}(\theta_f^k) + \psi_{f,m}(\theta_f^m)\Big] \xi_f a_f \Big\}$$

where:

$$\begin{aligned} \mu_a(a, c_f, \boldsymbol{\theta}_f, \boldsymbol{s}, g_h) &= \tilde{r}_f^n + \theta_f^k (\tilde{r}^k - \tilde{r}_f^n) + \theta_f^m (\tilde{r}_t^m - \tilde{r}_f^n) - c_{f,t}/a_f - \tau_f \\ \sigma_a(\boldsymbol{\theta}_f, \boldsymbol{s}, g_h) &= \theta_f^k \tilde{\sigma}_{q^k,z} + \theta_f^m \tilde{\sigma}_{q^m,z} + (1 - \theta_f^k - \theta_f^m) \tilde{\sigma}_{q^n,z} = \boldsymbol{\theta}_f^T \tilde{\boldsymbol{\sigma}}_{q,t} \end{aligned}$$

Following the same steps, the equilibrium FOCs for the fund are given by:

$$\begin{aligned} [c_f] &: \qquad 0 = u'(c_f) - \partial_a V_f(a, \cdot) \\ [\iota_f] &: \qquad 0 = \Phi'(\iota) - \frac{1}{q^k} \\ [\theta_f^k] &: \qquad 0 = r^k - r_f^n + \sigma_{\xi_f}(\sigma_{q^k,z} - \sigma_{q^n,z}) + \partial_{\theta_f^k} \psi_{f,k} \\ [\theta_f^m] &: \qquad 0 = r^m - r_f^n + \sigma_{\xi_f}(\sigma_{q^m,z} - \sigma_{q^n,z}) + \partial_{\theta_f^k} \psi_{f,m} \end{aligned}$$

and the Euler equation is:

$$\rho_f = \mu_{\xi_f} + r_f^n - \tau_h + \Big[\psi_{f,k} + \psi_{f,m} - \partial_{\theta_f^k} \psi_{f,k} \theta_f^k - \partial_{\theta_f^m} \psi_{f,m} \theta_f^m\Big] + \sigma_{q^n,z} \sigma_{\xi_f}$$

A.1.3 Equilibrium Functions

The agent optimization problem has the terms:

$$\xi_h(a, z, K, g), \quad D_x \xi_h(a, z, K, g) = \begin{bmatrix} \partial_a \xi_h(a, z, K, g) \\ \partial_z \xi_h(a, z, K, g) \\ \partial_K \xi_h(a, z, K, g) \\ \partial_{\eta_h} \xi_h(a, z, K, g) \\ \partial_{\eta_f} \xi_h(a, z, K, g) \end{bmatrix}$$

In equilibrium we have that that $a = \eta_h A(\boldsymbol{s})$ where $A(\boldsymbol{s}) = q^k(\boldsymbol{s})K + q^m(\boldsymbol{s})M$:

$$
\begin{aligned}
\Xi_h(z, g, K) &= \xi_h(a, z, K, g)|_{a=\eta_h A(\boldsymbol{s})} \\
\Xi_h'(z, g, K) &= D_x \xi_h(a, z, K, g)|_{a=\eta_h A(\boldsymbol{s})}
\end{aligned}
$$

The term $\Xi_i'(z, g, K)$ appears throughout the FOCs equations so we need approximate it. However, we have:

$$
\Xi_h'(z, g, K) \neq D_s \Xi_h(z, g, K)
$$

for the obvious reason that the dimension is different. Instead, we have that:

$$
D_s \Xi_h(z, g, K) = \begin{bmatrix} \partial_z \xi_h(\eta_h A(s), z, K, g) \\ \partial_\zeta \xi_h(\eta_h A(s) z, K, g) \\ \partial_K \xi_h(\eta_h A(s), z, K, g) \\ \partial_a \xi_h(a, z, K, g)|_{a=\eta_h A(s)} A(s) + \partial_{\eta_h} \xi_h(a, z, K, g)|_{a=\eta_h A(s)} \\ \partial_{\eta_f} \xi_h(\eta_h A(s), z, K, g) \end{bmatrix}
$$

Proposition 1. *In equilibrium, we have that for $j \in \{h, b, f\}$:*

$$
\begin{aligned}
\mu_{\xi_h} \xi_j(a, \boldsymbol{s})|_{a=\eta_j A(\boldsymbol{s})} &= \mu_{\Xi_j} \Xi_j(\boldsymbol{s}) \\
\sigma_{\xi_j} \xi_j(a, \boldsymbol{s})|_{a=\eta_j A(\boldsymbol{s})} &= \sigma_{\Xi_j} \Xi_j(\boldsymbol{s})
\end{aligned}
$$

Proof. For clarity, I show this in the non-matrix form for the household rather than using the matrix chain rule. For the volatility, we have that:

$$
\begin{aligned}
\sigma_{\xi_h} \xi_h &= (\boldsymbol{\sigma}_x \odot \boldsymbol{x})^T (D_x \xi_h) \\
&= \partial_a \xi_h \sigma_{a,z} a + \partial_z \xi_h \sigma_z z + \sum_j \partial_{\eta_j} \xi_h \sigma_{\eta_j, z} \eta_j
\end{aligned}
$$

After imposing equilibrium $a = \eta_1 A(\boldsymbol{s})$, where $A(\boldsymbol{s}) = q^k K + q^m M$, we have that the RHS is:

$$
\begin{aligned}
RHS &= \partial_a \xi_h \sigma_{a,z} \eta_1 A(\boldsymbol{s}) + \partial_z \xi_h \sigma_z z + \sum_j \partial_{\eta_j} \xi_h \sigma_{\eta_j,z} \eta_j \\
&= \begin{bmatrix} \sigma_{a,z} \\ \sigma_z \\ 0 \\ 0 \\ \sigma_{\eta_h,z} \\ \sigma_{\eta_f,z} \end{bmatrix}^T \begin{bmatrix} \partial_z \xi_h(\eta_h A(s), z, K, g) \\ \partial_\zeta \xi_h(\eta_h A(s) z, K, g) \\ \partial_K \xi_h(\eta_h A(s), z, K, g) \\ \partial_a \xi_h(\eta_h A(s), z, K, g) A(s) + \partial_{\eta_h} \xi_h(\eta_h A(s), z, K, g) \\ \partial_{\eta_f} \xi_h(\eta_h A(s), z, K, g) \end{bmatrix} \\
&= (\boldsymbol{\sigma}_s \odot \boldsymbol{s})^T (D_s \Xi_h) \\
&= \sigma_{\Xi_h} \Xi_h
\end{aligned}
$$

□

Equilibrium Portfolio Choice: Imposing Proposition 1 we have that the portfolio choices satisfy:

$$
\begin{aligned}
&[\theta_h^k]: & r^k - r^d =& -\lambda \partial_{\theta_h^k} \mathcal{W}(\theta_h^k, \theta_h^n) \frac{\mathcal{U}'(\mathcal{C})}{a \Xi_h} - \partial_{\theta_h^k} \psi_{h,k} - \sigma_{\Xi_h} \sigma_{q^k} \\
&[\theta_h^n]: & r_h^n - r^d =& -\lambda \partial_{\theta_h^n} \mathcal{W}(\theta_h^k, \theta_h^n) \frac{\mathcal{U}'(\mathcal{C})}{a \Xi_h} - \partial_{\theta_h^n} \psi_{h,n} - \sigma_{\Xi_h} \sigma_{q^n} \\
&[\theta_b^k]: & r^k - r^d =& -\sigma_{\Xi_b} \sigma_{q^k} - \partial_{\theta_b^k} \psi_{b,k} \\
&[\theta_b^m]: & r^m - r^d =& -\sigma_{\xi_b} \sigma_{q^m,z} - \partial_{\theta_b^m} \psi_{b,m} \\
&[\theta_f^k]: & r^k - r_f^n =& -\sigma_{\Xi_f} (\sigma_{q^k} - \sigma_{q^n}) \\
&[\theta_f^m]: & r^m - r_f^n =& -\sigma_{\Xi_f} (\sigma_{q^m} - \sigma_{q^n})
\end{aligned}
$$

where:

$$
r_f^n = r_h^n + \left(\frac{1}{q_t^n} - 1 \right) \lambda_h
$$

Equilibrium Euler Equations: Imposing Proposition 1 we have that the Euler equations satisfy:

$$\begin{aligned}
\rho_h + \lambda_h &= \mu_{\Xi_h} + r^d - \tau_h + \psi_{h,k}(\theta_h^k) - \partial_{\theta_h^k}\psi_{h,k}(\theta_h^k)\theta_h^k + \psi_{h,n}(\theta_h^n) - \partial_{\theta_h^n}\psi_{n,k}(\theta_h^n)\theta_h^n \\
\rho_b &= \mu_{\Xi_b} + r^d - \tau_b + \left[\psi_{b,k} + \psi_{b,m} - \partial_{\theta_b^k}\psi_{b,k}\theta_b^k - \partial_{\theta_b^m}\psi_{b,m}\theta_b^m\right] \\
\rho_f &= \mu_{\Xi_f} + r_f^n - \tau_f + \left[\psi_{f,k} + \psi_{f,m} - \partial_{\theta_f^k}\psi_{f,k}\theta_f^k - \partial_{\theta_f^m}\psi_{f,m}\theta_f^m\right] + \sigma_{q^n,z}\sigma_{\Xi_f}
\end{aligned}$$

A.1.4 Equilibrium Block 1: Summary of Optimization

Given equilibrium prices and price processes:

$$(r^d, q^k, r^k, \sigma_{q^k}, q^n, r^n, \sigma_{q^n}, q^m, r^m, \sigma_{q^m})$$

the household, banker, and fund optimization variables (14 variables):

$$(\Xi_h, \Xi_b, \Xi_f, c_h, \mathcal{C}_h, c_b, c_f, \theta_h^k, \theta_h^n, \theta_b^k, \theta_b^m, \theta_f^k, \theta_f^m, \iota)$$

satisfy the optimization equations (14 equations):

$$
\begin{aligned}
0 =& -(\rho_h + \lambda_h) + \mu_{\Xi_h} + r^d - \tau_h + \psi_{h,k}(\theta_h^k) - \partial_{\theta_h^k}\psi_{h,k}(\theta_h^k)\theta_h^k \\
&+ \psi_{h,n}(\theta_h^n) - \partial_{\theta_h^n}\psi_{n,k}(\theta_h^n)\theta_h^n \\
0 =& -\rho_b + \mu_{\Xi_b} + r^d - \tau_b + \left[\psi_{b,k} + \psi_{b,m} - \partial_{\theta_b^k}\psi_{b,k}\theta_b^k - \partial_{\theta_b^m}\psi_{b,m}\theta_b^m\right] \\
0 =& -\rho_f + \mu_{\Xi_f} + r_f^n - \tau_h + \left[\psi_{f,k} + \psi_{f,m} - \partial_{\theta_f^k}\psi_{f,k}\theta_f^k - \partial_{\theta_f^m}\psi_{f,m}\theta_f^m\right] + \sigma_{q^n,z}\sigma_{\Xi_f} \\
0 =& \, u'(c_h) - \Xi_h \\
0 =& \, u'(c_b) - \Xi_b \\
0 =& \, u'(c_f) - \Xi_f \\
0 =& -\mathcal{C}_h + a(\theta_h^k(1-\tau))^\alpha((q^n)^{-1}\theta_h^n)^{1-\alpha} \\
0 =& \, r^k - r^d + \lambda_h \partial_{\theta_h^k}\mathcal{W}(\theta_h^k, \theta_h^n)\frac{\mathcal{U}'(\mathcal{C})}{a\Xi_h} + \partial_{\theta_h^k}\psi_{h,k} + \sigma_{\Xi_h}\sigma_{q^k} \\
0 =& \, r^n - r^d + \lambda_h \partial_{\theta_h^n}\mathcal{W}(\theta_h^k, \theta_h^n)\frac{\mathcal{U}'(\mathcal{C})}{a\Xi_h} + \partial_{\theta_h^n}\psi_{h,n} + \sigma_{\Xi_h}\sigma_{q^n} \\
0 =& \, r^k - r^d + \sigma_{\Xi_b}\sigma_{q^k} + \partial_{\theta_b^k}\psi_{b,k} \\
0 =& \, r^m - r^d + \sigma_{\Xi_b}\sigma_{q^m} + \partial_{\theta_b^m}\psi_{b,m} \\
0 =& \, r^k - r_f^n + \sigma_{\Xi_f}(\sigma_{q^k} - \sigma_{q^n}) + \partial_{\theta_f^k}\psi_{f,k} \\
0 =& \, r^m - r_f^n + \sigma_{\Xi_f}(\sigma_{q^m} - \sigma_{q^n}) + \partial_{\theta_f^m}\psi_{f,m} \\
0 =& \, \Phi'(\iota) - \frac{1}{q^k}
\end{aligned}
$$

A.1.5 Equilibrium Block 2: Distribution Evolution

Kolmogorov Forward Equation (KFE): Financial Sector: We consider two levels of the distribution evolution. Let $A_{h,t}$, $A_{b,t}$, and $A_{f,t}$ denote the aggregate wealth in the household, banking, and fund sectors. Let $g_{j,t}$ denote the measure function of wealth for type $j \in \{h, b, f\}$.

We start with the evolution of aggregate wealth in the banking sector:

$$
\begin{aligned}
\frac{dA_{b,t}}{A_{b,t}} &= \frac{1}{A_{b,t}}\int_0^\infty \mu_{a_b}(c_h(a),\boldsymbol{\theta}_b,\boldsymbol{S})ag_{b,t}(a)dadt + \frac{1}{A_{b,t}}\lambda_b(\phi_b A_t - A_{b,t})dt \\
&\quad + \frac{1}{A_{b,t}}\int_0^\infty \sigma_{b,t}(\boldsymbol{\theta}_b,\boldsymbol{S})adW_t a g_{b,t}(a)da \\
&= \left(\mu_{a_b}(c_h(a),\boldsymbol{\theta}_b,\boldsymbol{S}) + \lambda_b\left(\frac{\phi_b}{\eta_{b,t}}-1\right)\right)dt + \sigma_{b,t}(\boldsymbol{\theta}_b,\boldsymbol{S})dW_t \\
&= \left(r^d + \theta_h^k(r^k - r^d) - (\rho_b + \lambda_b) - \tau_b + \lambda_b\left(\frac{\phi_b}{\eta_{b,t}}-1\right)\right)dt \\
&\quad + \sigma_{b,t}(\boldsymbol{\theta}_b,\boldsymbol{S})dW_t
\end{aligned}
$$

Likewise, the evolution of aggregate wealth in the fund section is:

$$
\begin{aligned}
\frac{dA_{f,t}}{A_{f,t}} = &\left(r^b + \theta_f^k(r^k - r_f^b) + \theta_f^m(r^m - r_f^n) - (\rho_f + \lambda_f) - \tau_f + \lambda_f\left(\frac{\phi_f}{\eta_{f,t}}-1\right)\right)dt \\
&+ \sigma_{f,t}(\boldsymbol{\theta}_f,\boldsymbol{S})dW_t
\end{aligned}
$$

Aggregate wealth is given by $A_t = q_t^k K_t + q_t^m M$. Let $\vartheta_t = q_t^k K_t/(q^k K_t + q^m M)$. The evolution of aggregate wealth follows:

$$
\begin{aligned}
\frac{dA_t}{A_t} &= \vartheta\left(\frac{dq^k}{q^k} + \frac{dK}{K}\right) + (1-\vartheta)\frac{dq^m}{q^m} \\
&= \underbrace{\vartheta(\mu_{q^k} + \Phi(\iota) - \delta) + (1-\vartheta)\mu_{q^m}}_{\mu_A} + \vartheta\sigma_{q^k,z}dW \\
&\quad + (1-\vartheta)\sigma_{q^m,z}dW_t
\end{aligned}
$$

So, the evolution of $\eta_{b,t} = A_{b,t}/A_t$ is given by:

$$
\begin{aligned}
\frac{d\eta_{b,t}}{\eta_{b,t}} &= \frac{dA_{b,t}}{A_{b,t}} - \frac{dA_t}{A_t} - \frac{dA_{b,t}}{A_{b,t}}\frac{dA_t}{A_t} + \left(\frac{dA_t}{A_t}\right)^2 \\
&= (\mu_{A_b,t} - \mu_{A,t} - \sigma_{A_b,t}\sigma_{A,t} + \sigma_{A,t}\sigma_{A,t})\,dt + (\sigma_{A_b,t} - \sigma_{A,t})dW_t \\
&= (\mu_{A_b,t} - \mu_{A,t} + (\sigma_{A,t} - \sigma_{A_b,t})\sigma_{A,t})\,dt + (\sigma_{A_b,t} - \sigma_{A,t})dW_t
\end{aligned}
$$

and the evolution of $\eta_{f,t} = A_{f,t}/A_t$ is given by:

$$
\frac{d\eta_{f,t}}{\eta_{f,t}} = \left(\mu_{A_f,t} - \mu_{A,t} + (\sigma_{A,t} - \sigma_{A_f,t})\sigma_{A,t}\right)dt + (\sigma_{A_f,t} - \sigma_{A,t})dW_t
$$

KFE: Within Households: The KFE for the household distribution in levels, a, is given by:

$$
\begin{aligned}
dg_{h,t}(a) = & + \lambda_h \phi(a) A_t - \lambda_h g_{h,t}(a) - \partial_a[\mu_a(a, \boldsymbol{s}_t, g_{h,t}) g_{h,t}(a)] \\
& - \partial_a[\sigma_a(a, \boldsymbol{s}_t, g_{h,t}) dW_t g_{h,t}(a)] + \frac{1}{2}\partial_a \left[\boldsymbol{\sigma}_a^T \boldsymbol{\sigma}_a(a, \boldsymbol{s}_t, g_{h,t}) g_{h,t}(a)\right] dt \\
= & + \lambda_h \phi(a) A_t - \lambda_h g_{h,t}(a) - \partial_a[\mu_a(a, \boldsymbol{s}_t, g_{h,t}) g_{h,t}(a)] \\
& - \partial_a[\sigma_{a,z}(a, \boldsymbol{s}_t, g_{h,t}) g_{h,t}(a)] dW_{z,t} \\
& + \frac{1}{2}\partial_a \left[(\sigma_{a,z}^2(a, \boldsymbol{s}_t, g_{h,t})) g_{h,t}(a)\right] dt
\end{aligned}
$$

The evolution $\eta_{i,t} := a_{i,t}/A_t$ is given by:

$$
\begin{aligned}
\frac{d\eta_{i,t}}{\eta_{i,t}} = & \ (\mu_{a_i,t} - \mu_{A,t} + (\sigma_{A,t} - \sigma_{a_i,t}) \boldsymbol{\sigma}_{A,t})\, dt + (\sigma_{a_i,t} - \sigma_{A,t}) dW_t \\
=: & \ \mu_{\eta_i,t} dt + \sigma_{\eta_i,t} dW_t
\end{aligned}
$$

where we have softened the entry function from ϕ_h to $\phi(a)$, where $\phi(a)$ is a function with mean ϕ_h. For a, a natural candidate would be $\phi(a) = \text{LogNormal}(\phi_h, \sigma)$. Likewise, the KFE for the distribution in shares is:

$$
\begin{aligned}
dg_{h,t}(\eta) = & + \lambda_h \phi(\eta) - \lambda_h g_{h,t}(\eta) - \partial_\eta[\mu_\eta(\eta, \boldsymbol{s}_t, g_{h,t}) g_{h,t}(\eta)] \\
& - \partial_\eta[\sigma_\eta(\eta, \boldsymbol{s}_t, g_{h,t}) dW_t g_{h,t}(\eta)] + \frac{1}{2}\partial_\eta \left[\boldsymbol{\sigma}_\eta^T \boldsymbol{\sigma}_\eta(\eta, \boldsymbol{s}_t, g_{h,t}) g_{h,t}(\eta)\right] dt \\
= & + \lambda_h \phi(\eta) - \lambda_h g_{h,t}(\eta) - \partial_\eta[\mu_\eta(\eta, \boldsymbol{s}_t, g_{h,t}) g_{h,t}(\eta)] \\
& - \partial_\eta[\sigma_{\eta,z}(\eta, \boldsymbol{s}_t, g_{h,t}) g_{h,t}(\eta)] dW_{z,t} \\
& + \frac{1}{2}\partial_\eta \left[(\sigma_{\eta,z}^2(\eta, \boldsymbol{s}_t, g_{h,t}) + \sigma_{\eta,\zeta}^2(\eta, \boldsymbol{s}_t, g_{h,t})) g_{h,t}(\eta)\right] dt
\end{aligned}
$$

where again we have softened the entry function ϕ_h to $\phi(\eta)$, where $\phi(\eta)$ is a function with mean ϕ_h. For η, a natural candidate would be $\phi(\eta) \sim$ Beta with mean ϕ_h.

B Algorithm

Figure 5 presents the average HJB error in marginal utility units over epochs along with the 95% confidence interval across 10 runs with different seeds. The algorithm converges successfully with sufficiently small deviations across different runs. The error saturates after 50k epochs where gradient norm of all neural network parameters stabilizes.

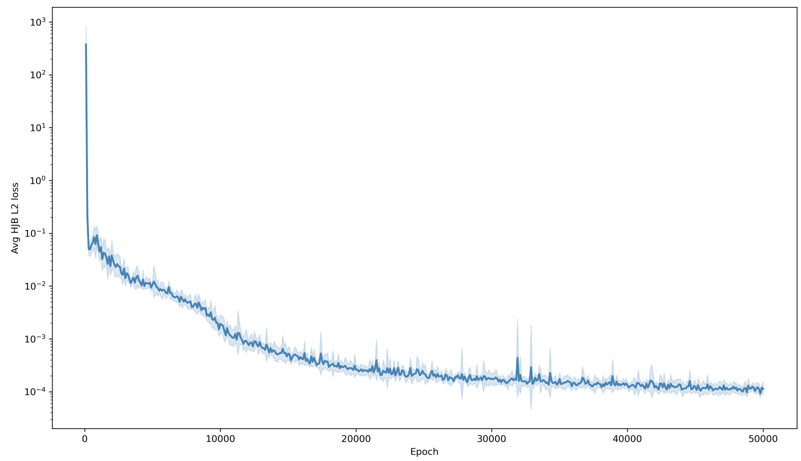

Figure 5: The total average L-2 loss from the quantitative model over iterations on a logarithmic scale. The neural network architecture is 2 hidden layers with 256 neurons in each layer trained using an ADAM optimizer. The shaded area represent 95% confidence interval over 10 different runs with different seeds.

C Additional Details on Simulating

In order to simulate the economy we need to compute the evolution of the household wealth distribution. This is complicated for the finite agent approximation method because the neural network policy rules are functions of the positions of the N other agents rather than a continuous density. To overcome this difficulty, we deploy the "hybrid" approach described in Algorithm 2 that uses the neural network solution to approximate a finite difference approximation to the KFE. Let $\underline{\boldsymbol{a}} = (a_m : m \leq M)$ denote the grid in the a-dimension. Let $\underline{\boldsymbol{g}}_t = (g_{m,t} : m \leq M)$ denote the marginal density on the a-grid. At each time step, our method draws N_{sim} different samples of N agents from from the current density g_t. For each draw $k \leq N_{sim}$, denoted by $\hat{\varphi}_t^k = (a_i : 1 \leq i \leq N)$, the KFE is replaced by the following finite difference equation:

$$dg_{m,t} = \mu_{g,m}(\hat{\varphi}_t^k)dt + \boldsymbol{\sigma}_{g,m}^T(\hat{\varphi}_t^k)d\boldsymbol{W}_t, \qquad m \leq M \tag{C.1}$$

where the drift at point (m) is defined by the finite difference approximation for the KFE using the policy rules from our finite population neural network solution. From this approximation we can calculate the transition matrix $\mathcal{A}_{t,k}$ for the finite difference approximation at the draw φ^k. We repeat this procedure many times then compute an average transition matrix, which we use for simulation. We summarize the steps in Algorithm 2.

Algorithm 2: Finding Transition Paths In Finite Agent Approximation

Input : Initial distribution, neural network approximations to the policy and price functions, number of agents N, time step size Δt, number of time steps N_T, number of simulations N_{sim}, grid $\underline{\boldsymbol{a}} = \{a_m : m \leq M\}$ for the finite difference approximation.

Output: A transition path $g = \{g_t : t = 0, \Delta t, \ldots, N_T \Delta t\}$

for $n = 0, \ldots, N_T - 1$ **do**
  for $k = 1, \ldots, N_{sim}$ **do**
    Sample $\Delta W_{t,z}$ from the normal distribution $N(0, \Delta t)$, construct TFP shock paths by: $z_{t+\Delta t} = z_t + \eta(\bar{z} - z_t) + \sigma \Delta B_t^0$. Do likewise to construct the volatility shock path.
    Draw states for N agents $\{\varphi_i^k : i = 1, \ldots, N\}$ from density g_t at $t = n\Delta t$.
    Given state $(z_{t+\Delta t}, \varphi_t^k)$, compute equilibrium prices and returns.
    At each grid point $a_m \in \underline{\boldsymbol{a}}$, calculate the consumption and portfolio choices.
    Construct the transition matrix $\mathcal{A}_{t,k}$ using finite difference on the grid $\underline{\boldsymbol{a}}$, as described by (C.1).
  end
  Take the average: $\bar{\mathcal{A}}_t = \frac{1}{N_{sim}} \sum_{k=1}^{N_{sim}} \mathcal{A}_{t,k}$
  Update g_t by implicit method: $g_{t+\Delta t} = (I - \bar{\mathcal{A}}_t^\top \Delta t)^{-1} g_t + \boldsymbol{\sigma}^T d\boldsymbol{W}_{t,z}$
end

C.1 Multiple stochastic steady states

Our model admits multiple stochastic steady states. Figure 6 displays the drift of the bank's wealth share as a function of its own wealth share. We sample 2000 points from the state space and compute the equilibrium drift using the evolution equation in Theorem 2 in two economies: the baseline economy and an alternate economy where households' demand for deposits dominates other assets. For illustration, we fit a cubic spline curve to the scatter points. In the baseline economy, there is a non-degenerate stationary density around $\eta_b = 0.23$, as evidenced by the drift curve crossing zero at that point. In the alternate economy, the drift is increasing in the bank's wealth share, implying that the bank takes over the economy in the long run.

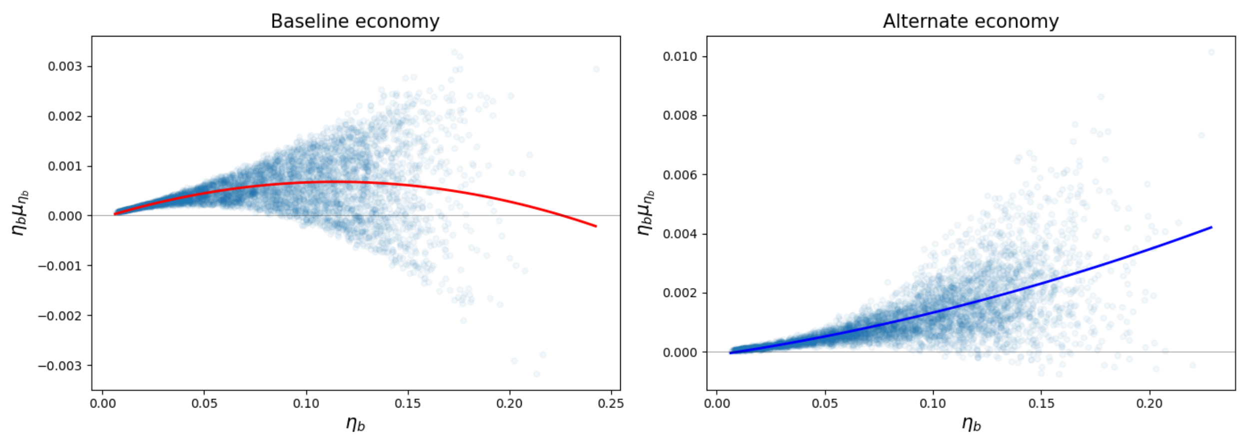

Figure 6: The left panel plots the drift of bank's wealth share as a function of η_b in the baseline economy. The right panel plot the same in an alternative economy with high household deposit demand. In both panels, scatter points represent the equilibrium drift from a sample of 2000 randomly drawn points from the state space. The red and blue line represent a cubic spline fit to the points.

D Online Appendix

We "test" our approach by using our algorithm to characterize the solution to three macro-finance models that can be solved using conventional methods: a complete markets model, Basak and Cuoco (1998), and Brunnermeier and Sannikov (2014). First we summarize the key results, and then present the model details. For all models, we use simple feed-forward neural networks and an ADAM optimizer. The details of the neural network parameters for each model are shown in Table 6.

Model	Num of Layers	Num of Neurons	Learning Rate
"As-if" Complete Model	4	64	0.001
Limited Participation Model	5	64	0.001
BruSan Model	5	32	0.001

Table 6: Neural network parameters for the three testible models

Table 7 summarizes the mean squared error between the conventional solution and the neural network solution. Evidently, the neural network and conventional methods converge to very similar characterizations of equilibrium. Each following subsection describes how the model in that section can be nested with the main model along with technical details.

Method	L1-Error
Complete markets	1.0×10^{-5}
Basak and Cuoco (1998)	4.9×10^{-4}
Brunnermeier and Sannikov (2014)	7.0×10^{-5}

Table 7: Summary of the algorithm performance and computational speed. Error calculates the difference between solution by neural network and finite difference. All errors are in absolute value (L1).

D.1 Complete Market Model

We make the following modifications to map our N agent segmentation model from the main text to a Lucas Tree model. We set both the capital depreciation rate δ and the capital participation constraint function to zero. We fix the capital level K_t to be one and remove all portfolio penalty functions. To further simplify our notations, we introduce the output level $y_t = e^{z_t}$. Without financial frictions, there is simple aggregation of individuals'

Euler equations, which coincides with the representative agent's pricing equation. Let us assume that y_t follows a geometric Brownian motion process.

$$dy_t = \mu y_t dt + \sigma y_t dW_t^0.$$

Analytical Solution. In a representative agent's world, by the standard Lucas tree pricing formula, the asset price is determined by the discounted flow of dividends:

$$q(y_0) = \mathbb{E}\left[\int_0^\infty e^{-\rho t}\frac{u'(c_t)}{u'(c_0)}y_t dt\right] = y_0\mathbb{E}\left[\int_0^\infty e^{-\rho t}(y_t/y_0)^{1-\gamma}dt\right]$$

Note that for geometric Brownian motion, the distribution of output is given by:

$$\ln(y_t/y_0) \sim \mathcal{N}\left((\mu - \frac{1}{2}\sigma^2)t, \sigma^2 t\right)$$

which means (the integral and expectation operator are interchangeable):

$$\begin{aligned}
\mathbb{E}(y_t/y_0)^{1-\gamma} &= (1-\gamma)(\mu - \frac{1}{2}\sigma^2)t + \frac{1}{2}(1-\gamma)^2\sigma^2 t \\
&= (1-\gamma)\mu t + \frac{1}{2}(\gamma-1)\gamma\sigma^2 t \\
&\equiv -\breve{g}t
\end{aligned}$$

Therefore, asset prices are given by:

$$q(y_0) = y_0\int_0^\infty e^{-\rho t}e^{-\breve{g}t}dt = \frac{y_0}{\rho + \breve{g}} = \frac{y_0}{\rho + (\gamma-1)\mu - \frac{1}{2}\gamma(\gamma-1)\sigma^2}$$

By goods market clearing condition, we know that $c_t = y_t$, which means that the consumption policy is:

$$c = \left[\rho + (\gamma-1)\mu - \frac{1}{2}\gamma(\gamma-1)\sigma^2\right]q$$

For $\gamma = 5, \mu = 0.02, \sigma = 0.05, \rho = 0.05$ in the numerical example, $c/q = 10.5\%$, which means: $q(1) = 1/10.5\% \approx 9.5$.

Neural Network Solution. Though aggregation results hold, we still incorporate the wealth heterogeneity in our solution algorithm, i.e., we have N asset pricing conditions and N Euler equations. We compare the equilibrium asset price $q(\cdot, y)$ and consumption to wealth ratio $\omega_i(\cdot, y)$ with the "as-if" representative agent economy. The estimated time cost for the

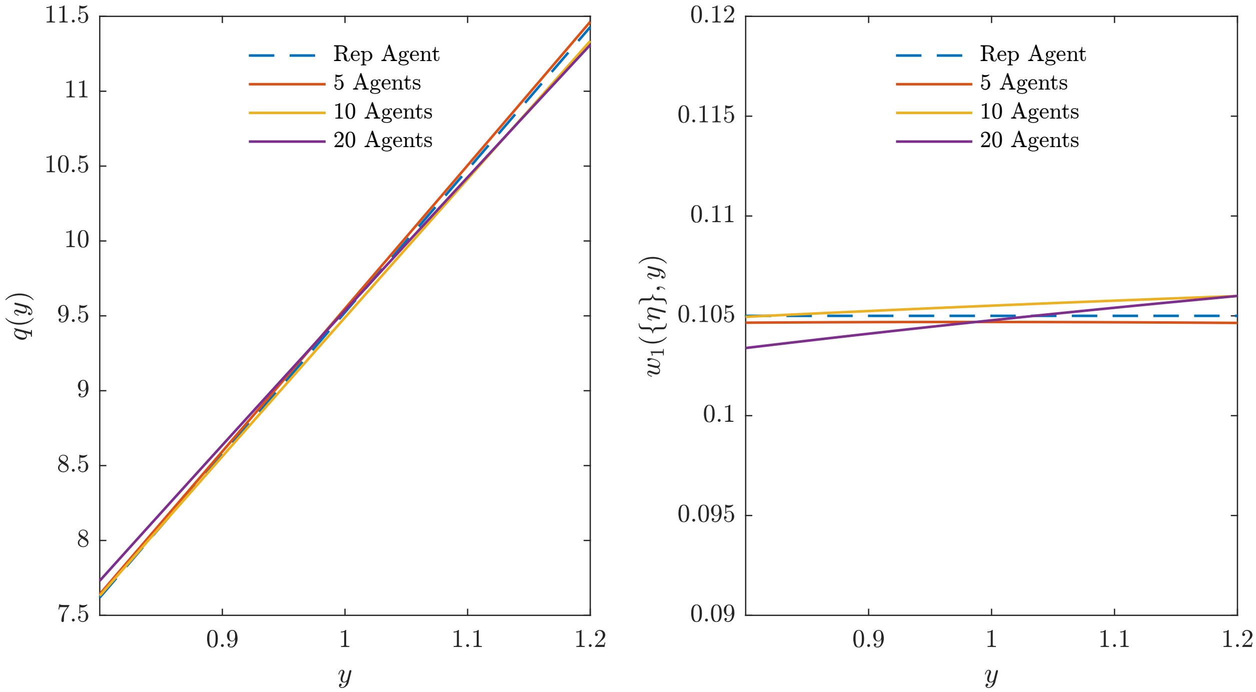

Figure 7: Solution to As-if representative agent model. Right panel: consumption-wealth ratio of agent 1.

model with 5, 10, and 20 agents is about 2 mins, 10 mins, and 20 mins, respectively. The difference between the consumption rule solved using our neural network method and the analytical solution is less than 0.1% for 5 and 10 agents, and 0.5% for 20 agents, respectively. The parameters for the complete market model are provided in Table 9.

Num of Agents	Euler Eq Error	Diff	Time Cost
5	<1e-4	<0.1%	2 mins
10	<1e-4	<0.5%	10 mins
20	<1e-3	<0.5%	20 mins

Table 8: Summary of the algorithm performance and computational speed. "Diff" means the difference between representative agent case's solution and brute-force. All errors are in absolute value (L1 loss).

Parameter	Symbol	Value
Risk aversion	γ	5.0
Agents' Discount rate	ρ	0.05
Output Growth Rate	μ	2%
Volatility of Growth	σ	5%

Table 9: Model parameters.

D.2 Asset Pricing with Restricted Participation

We carry forward modifications to the main model from the previous section to mimic the endowment economy. Consider an infinite-horizon economy with two types of price-taking agents: expert (indexed by e) and household (indexed by h). The financial friction is that households cannot participate in the capital market. Experts do not face this constraint. Mathematically, it is stated as

$$\Psi_i(a_i, b_i) = -\frac{\bar{\psi}_i}{2}(a_i - b_i)^2, \bar{\psi}_h = \infty, \bar{\psi}_e = 0.$$

As before, the output y_t follows a geometric Brownian motion process.

$$dy_t = \mu y_t dt + \sigma y_t dZ_t.$$

Finite Difference Solution. We exploit the scalability for geometric Brownian motion's case to get a precise solution by focusing on one-dimensional differential equation. For a scalable income process, we postulate the price function as $q = f(\eta)y$, where η is the expert's wealth share with no loss of generality, i.e., $\eta = \eta_e$ (and $1 - \eta = \eta_h$). The value function can be written as:

$$V_i = \frac{1}{\rho_i}\frac{(\omega_i \eta_i q)^{1-\gamma}}{1-\gamma} = \frac{(\omega_i \eta_i f(\eta))^{1-\gamma}}{\rho_i}\frac{y^{1-\gamma}}{1-\gamma} \equiv v_i \frac{y^{1-\gamma}}{1-\gamma}, \quad i = e, h$$

where v_i is the scaled value function. From the first-order condition, we get [10]

$$c_i^{-\gamma} = \frac{1}{\rho_i}\frac{(\omega_i \eta_i q)^{1-\gamma}}{\eta_i q} \Rightarrow \left(\frac{c_i}{y}\right)^{\gamma} = \frac{\eta_i f(\eta)}{v_i}, \omega_i = [\eta_i f(\eta)]^{\frac{1}{\gamma}-1} v_i^{-\frac{1}{\gamma}}$$

[10] This expression leads to the boundary condition at $\eta = 1$: $\frac{f(1)}{v_e} = 1$

From the goods market clearing condition, we have:

$$1 = \frac{\sum_i c_i}{y} = \sum_i \left(\frac{\eta_i f(\eta)}{v_i}\right)^{\frac{1}{\gamma}} = y \Rightarrow f(\eta) = \frac{1}{\left[\sum_i \left(\frac{\eta_i}{v_i}\right)^{\frac{1}{\gamma}}\right]^{\gamma}} \tag{D.1}$$

The *HJB equation* for the scaled value function v_i is given by

$$[\rho_i - (1-\gamma)\mu + \frac{\gamma}{2}(1-\gamma)\sigma^2 - \omega_i]v_i = [\mu_\eta + (1-\gamma)\sigma\sigma_\eta]\eta\frac{\partial v_i}{\partial \eta} + \frac{1}{2}\frac{\partial^2 v_i}{\partial \eta^2}\eta^2\sigma_\eta^2 \tag{D.2}$$

where μ_η, σ_η's expressions are as follows.

$$\begin{aligned}\mu_\eta =& (1-\eta)(\omega_h - \omega_e) + \left(-\frac{1-\eta}{\eta}\right)(r_f - r_q + (\sigma_q)^2)\\ \sigma_\eta =& \frac{1-\eta}{\eta}\sigma_q, \text{where } r_f - r_q = \sigma_\xi\sigma_q, \quad \sigma_q = \frac{\sigma}{1 - \frac{f'(\eta)}{f(\eta)}(1-\eta)}.\end{aligned}$$

The price of risk which appears in the asset pricing condition is determined by Itô's Lemma as follows.

$$\xi_i = \frac{v_i}{\eta_i f(\eta)}y^{-\gamma} \Rightarrow \sigma_\xi = \sigma_v - \sigma_f - \sigma_\eta - \gamma\sigma = \frac{v_i'(\eta)\eta\sigma_\eta}{v_i} - \frac{f'(\eta)\eta\sigma_\eta}{f} - \sigma_\eta - \gamma\sigma.$$

In finite difference solution approach, we introduce a pseudo time-derivative. (D.2):

$$[\rho_i - (1-\gamma)\mu + \frac{\gamma}{2}(1-\gamma)\sigma^2 - \omega_i]v_i = [\mu_\eta + (1-\gamma)\sigma\sigma_\eta]\eta\frac{\partial v_i}{\partial \eta} + \frac{1}{2}\frac{\partial^2 v_i}{\partial \eta^2}\eta^2\sigma_\eta^2 + \frac{\partial v_i}{\partial t}$$

We then update the value function in an implicit scheme to solve the following equation.

$$\check{\boldsymbol{\rho}}\mathbf{I}\mathbf{v}_{t+dt} = \mathbf{M}\mathbf{v}_{t+dt} + \frac{\mathbf{v}_{t+dt} - \mathbf{v}_t}{dt},$$

where $\mathbf{M}$ is the differential matrix by upwind scheme, and $\mathbf{I}$ is the identity matrix.

Boundary Conditions. We focus on the case that $\eta \in (0,1]$, as the economy is ill-defined when experts are wiped out from the economy, i.e., there will be nobody left in the economy to hold the tree in equilibrium. To get the right boundary, we use the asset prices and consumption policy ω_e from the representative agent's solution:

$$\omega_e(1,y) = \rho_e + (\gamma-1)\mu - \frac{1}{2}\gamma(\gamma-1)\sigma^2, q(1,y) = \frac{y}{\omega_e(1,y)},$$

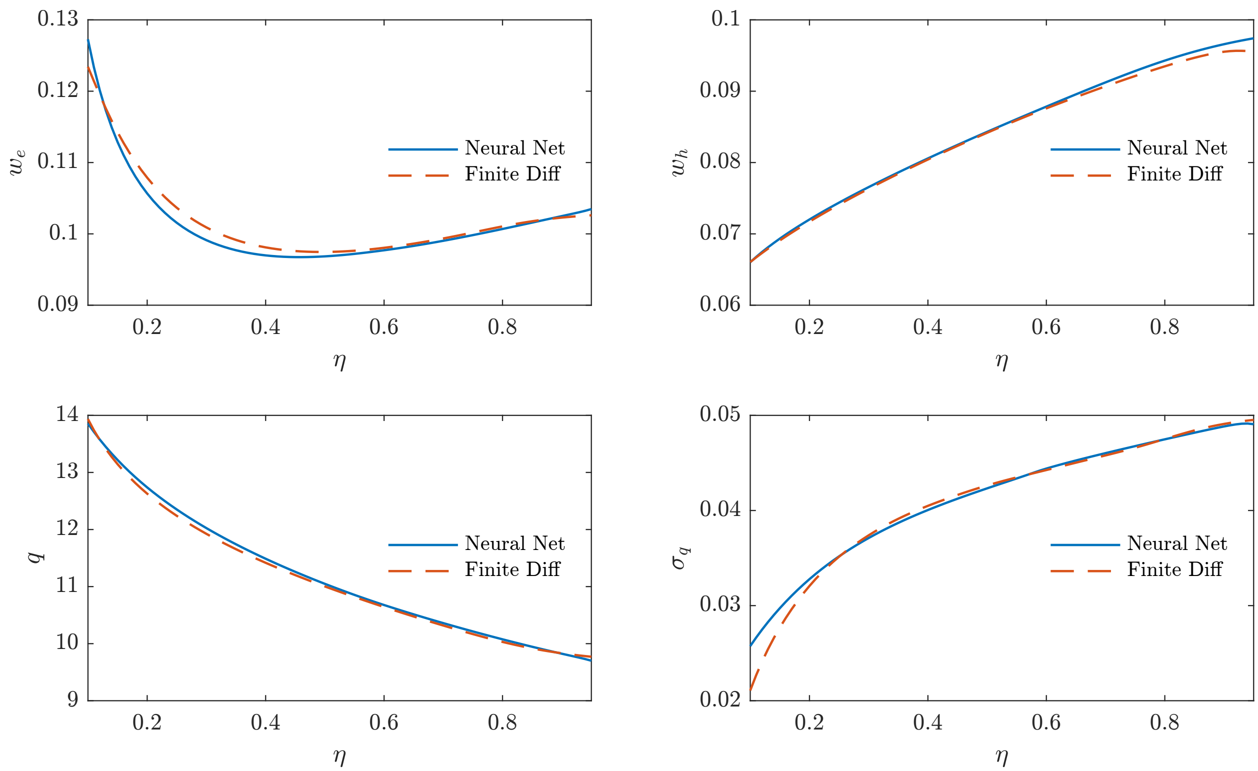

Figure 8: Solution to restricted stock market participation model.

which implies the boundary condition: $v_e(1) = \frac{1}{\rho_e+(\gamma-1)\mu-\frac{1}{2}\gamma(\gamma-1)\sigma^2}$.

The estimated time to solve the limited participation problem by neural network is about 5 minutes. We compare the finite difference solution with the neural network solution on η's dimension in figure 8 for $y = 1$. We can see that our method well captures the high non-linearity (left-upper panel) and amplification (right-lower panel). The parameters are provided in Table 10.

Parameter	Symbol	Value
Risk aversion	γ	5.0
Households' Discount rate	ρ_h	0.05
Experts' Discount rate	ρ_h	0.05
Output Growth Rate	μ	2%
Volatility of Growth	σ	5%

Table 10: Parameters for the restricted participation model.

D.3 A Macroeconomic Model with Productivity Gap

The setup in this example follows Brunnermeier and Sannikov (2016). There are two types of agents in this infinite horizon economy: experts and households. Both types can hold capital, but experts have a higher productivity rate compared to households. The productivity rates are given by z_h, z_e ($z_h < z_e$), respectively. Their relative risk aversions are the same, denoted by γ. Output grows exogenously by $\mu_y = y\mu$, with volatility $y\sigma$, and experts cannot issue outside equities. In addition, we assume that households cannot short capital, which can be formally written as:

$$\begin{cases} \Psi_h(a_h, b_h) = -\frac{\bar{\psi}_h}{2}(\min\{a_h - b_h, 0\})^2, & \bar{\psi}_h = \infty \\ \Psi_e(a_e, b_e) = -\frac{\bar{\psi}_e}{2}(a_e - b_e)^2, & \bar{\psi}_e = 0. \end{cases}$$

The output flow of households and experts follow

$$d_{e,t} = z_e y_t, d_{h,t} = z_h y_t, dy_t = y_t \mu dt + y_t \sigma dZ_t$$

The expected capital return is

$$r_{q,e,t} = \frac{d_{e,t}}{q_t} + \mu_{q,t}, r_{q,h,t} = \frac{d_{h,t}}{q_t} + \mu_{q,t}.$$

We rewrite the financial friction as the difference : $\frac{y_e - y_h}{q\sigma_q}$. For the first two equations, we have:

$$\begin{cases} -\frac{1}{\xi_e}\frac{\partial \xi_e}{\partial y}\sigma_y = \frac{1}{\xi_e}\frac{\partial \xi_e}{\partial \eta}\sigma_\eta - \frac{r_f - r_{q,h}}{\sigma_q} + \frac{y_e - y_h}{q\sigma_q} \\ -\frac{1}{\xi_h}\frac{\partial \xi_h}{\partial y}\sigma_y = \frac{1}{\xi_h}\frac{\partial \xi_h}{\partial \eta}\sigma_\eta - \frac{r_f - r_{q,h}}{\sigma_q} \end{cases}$$

Unlike the fully restricted participation's case where the experts hold all capital, we have to keep track of the capital allocation ratio of experts κ, which is parameterized as $\kappa = \eta + \lambda = \eta + \mathcal{N}_\lambda \eta^\beta$, where $\mathcal{N}_\lambda$ is a trainable neural network, and $\beta = \frac{1}{2}$ captures the power law for $\eta \to 0$. Given the expert's capital share holding κ, the volatility of wealth share σ_η is $(\kappa - \eta)\sigma_q$. The goods market clearing condition (D.1) is replaced by

$$f(\eta) = \frac{\kappa\eta z_e + (1-\kappa)(1-\eta)z_h}{\left[\sum_i \left(\frac{\eta_i}{v_i}\right)^{\frac{1}{\gamma}}\right]^\gamma}$$

and the price volatility is revised as

$$\sigma_q = \frac{\sigma}{1 - \frac{f'(\eta)}{f(\eta)}(\kappa - \eta)}$$

At the left boundary, $f(\cdot)$ is determined by $f(0) = \frac{y_h}{\omega_h(0)}$, $f(1) = \frac{y_e}{\omega_e(1)}$.

The estimated time to solve the model by our neural network method is about 5 minutes. Again, we compare the finite difference solution with the neural network solution in figure 9 for $y = 1$. We restrict the range of η to be the crisis region in Brunnermeier and Sannikov (2016), which is defined by the region where the capital share of experts $\kappa < 1$. This region captures the fire-sale region, where amplification takes place. We can see that the neural network solution well captures most of the amplification in that crisis region. The parameters are provided in Table 11.

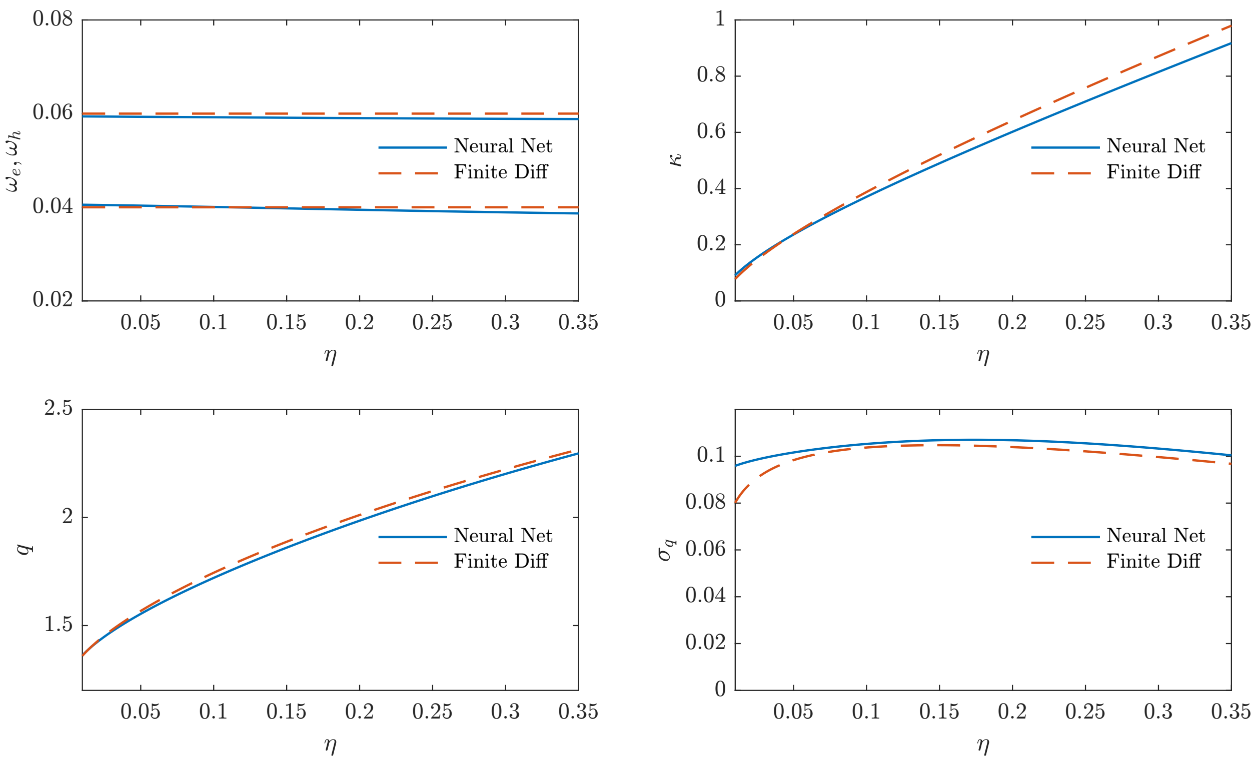

Figure 9: Solution to the model with productivity gap.

Parameter	Symbol	Value
Risk aversion	γ	1.0
Households' Discount rate	ρ_h	0.04
Experts' Discount rate	ρ_e	0.06
Households' Productivity	z_e	0.11
Experts' Productivity	z_h	0.05
Output Growth Rate	μ	2%
Volatility of Growth	σ	5%

Table 11: Parameters for the macroeconomic model.